DYNAMICAL EVOLUTION OF CLUSTERS OF GALAXIES, I

S. J. Aarseth

(Communicated by F. Hoyle)

(Received 1962 November 12)

Summary

Numerical integrations of the classical N-body problem have been carried out on a fast computer for a variety of clusters in the range $N=25$ to $N=100$. Newtonian forces are slightly modified to give convergence for collisions. The solutions are completely general and the results are applied to clusters of galaxies. It is found that the moment of inertia increases considerably even if bodies are not lost by ejection. At the same time there is an increase of mass in the central regions. The derived relaxation times are substantially longer than predicted by the theory of Chandrasekhar, but even so there is a deficiency of escapers for $N \gtrsim 50$. Some of the light cluster members are lost when the effect of cosmic expansion is included.

The dynamical formation rate of binaries is found to be small but this is compensated by long life-times for heavy doubles. Radially contracting clusters of irregular shapes are studied and a common feature is the formation of a compact sub-system of high stability. Field galaxies moving through a cluster do not affect the bound members significantly, but there is a likelihood of capture.

In some cases the integration time corresponds to a physical time $\sim 10^{10}$ yrs for a typical model cluster, but maximum errors in total energy may still be $\lesssim 0{\cdot}5$ per cent. The estimated computer time depends on the expression N^2t where t is the physical integration time.

---

1. *Introduction.*—Originally most clusters of galaxies were studied because they provide yard-sticks in the mapping of space. It is now realized that the clues to galaxy formation lie hidden in these island universes and more intensive studies of all their physical properties are being undertaken. Recent work by Abell (1) indicates that there are many different types of clusters, but the most numerous groups are found to contain around 50 visible bright galaxies. In the present paper we are interested in the dynamical behaviour of galaxies as they move about in a cluster and the effect this has on its large-scale evolution.

Given positions, velocities and masses for all cluster members and that the motions are governed by Newton's law, the future coordinates are in principle determined, provided the system is left to itself. Direct solutions of the N-body problem, however, have only been made possible by the introduction of high-speed computers. von Hoerner* (2) has given extensive results of numerical integrations for $N \leqq 16$, but since then faster computers have become available. One can argue that these results cannot be applied to cases where N is large, say, $N > 1000$. The effects due to individual encounters will be much larger when N is small, and this cannot be smoothed out by doing many cases which only eliminates statistical fluctuations.

* The results of two cases with $N=25$ integrated many relaxation times have been published in *Zs. f. Astrophys.*, **57**, 47, 1963.

For a given machine time one must compromise between the number of bodies to be integrated and the total integration time. Dynamically clusters of galaxies and open star clusters offer the best opportunities, firstly, because N is not too large and secondly, because their ages may be comparable to the relaxation times. The equations of motion will be slightly modified to take into account the force from extended bodies and we will in the following have in mind clusters of galaxies when results are discussed, even though the treatment is general.

2. *Theory.*—For the solution of the classical N-body problem as applied to clusters of galaxies we make the following assumptions:

(i) the forces are gravitational, apart from a possible cosmological expansion effect;

(ii) the total mass is distributed in the galaxies.

It has been suspected that clusters of galaxies contain considerable amounts of primeval matter, but as there is no definite evidence of this at the present time no such effect will be included. Moreover, the general force field will only be slightly less irregular if some of the mass is taken to be in the form of smoothed-out matter.

(iii) Individual masses remain constant ;

(iv) the Newtonian potential is slightly modified.

Galaxies are extended bodies but can generally be regarded as mass points. When two galaxies are involved in a collision, however, this is no longer a good approximation, because the forces are not convergent. To account for this, we take the potential due to the mass M at distance R to be

$$\Phi = \frac{GM}{[R^2+\xi^2]^{1/2}} \tag{1}$$

where ξ is a constant small distance, later to be associated with the effective size of a galaxy, and G is the gravitational constant.

The equation of motion for the ith body in an assembly of N interacting bodies can formally be written as,

$$\frac{d^2\mathbf{R}_i}{dt^2} = G\sum_{j=1}^{N}\frac{M_j(\mathbf{R}_j-\mathbf{R}_i)}{[|\mathbf{R}_j-\mathbf{R}_i|^2+\xi^2]^{3/2}} + H^2\mathbf{R}_i \tag{2}$$

where H is Hubble's constant. The expansion force $H^2\mathbf{R}_i$ is present for clusters of galaxies only in the steady-state and Lemaitre cosmological models. According to eqn. (2) the maximum force between two galaxies occurs at a distance $R=\xi/\sqrt{2}$.

We now introduce the dimensionless quantities m, r, τ, ϵ, and h for mass, distance, time, cut-off distance, and Hubble's constant respectively and write eqn. (2) in scaled form as

$$\frac{d^2\mathbf{r}_i}{d\tau^2} = \sum_{j=1}^{N}\frac{m_j(\mathbf{r}_j-\mathbf{r}_i)}{[|\mathbf{r}_j-\mathbf{r}_i|^2+\epsilon^2]^{3/2}} + h^2\mathbf{r}_i. \tag{3}$$

This implies the relations

$$\tau = G^{1/2}\left(\frac{r_i}{R_i}\right)^{3/2}\left(\frac{M_i}{m_i}\right)^{1/2} t \tag{4a}$$

$$h = \frac{t}{\tau}H, \quad \epsilon = \frac{r_i}{R_i}\xi. \tag{4b}$$

We write the virial theorem in the form

$$\sum_{i=1}^{N} M_i \left(\frac{d\mathbf{R}_i}{dt}\right)^2 = gG \sum_{i,j=1}^{N} \frac{M_i M_j |\mathbf{R}_j - \mathbf{R}_i|^2}{[|\mathbf{R}_j - \mathbf{R}_i|^2 + \xi^2]^{3/2}} \tag{5}$$

so that for $g = 0{\cdot}50$ the condition for statistical equilibrium is satisfied, provided the velocity distribution is isotropic. In terms of the scaled quantities

$$\sum_{i=1}^{N} m_i \left(\frac{d\mathbf{r}_i}{d\tau}\right)^2 = g \sum_{i,j=1}^{N} \frac{m_i m_j |\mathbf{r}_j - \mathbf{r}_i|^2}{[|\mathbf{r}_j - \mathbf{r}_i|^2 + \epsilon^2]^{3/2}} \equiv gV \tag{6}$$

where the virial $\frac{1}{2}V$ differs only slightly from the potential energy of the system. The coordinate system is taken to coincide with the centre of mass and we must therefore have

$$\sum_{i=1}^{N} m_i \mathbf{r}_i = 0, \quad \sum_{i=1}^{N} m_i \frac{d\mathbf{R}_i}{dt} = 0. \tag{7}$$

Furthermore, it is convenient to have mean mass and mean distance equal to unity, viz.

$$\sum_{i=1}^{N} m_i = N, \quad \sum_{i=1}^{N} r_i = N. \tag{8}$$

It now remains for the velocities to be scaled so that (6) shall be satisfied for the value of g specified, this is realized by putting

$$\frac{d\mathbf{r}_i}{d\tau} = \left[\frac{gV}{\sum m_i \left(\frac{d\mathbf{R}_i}{dt}\right)^2}\right]^{1/2} \frac{d\mathbf{R}_i}{dt}. \tag{9}$$

Finally, it is useful to have the axis of mean rotation (if any) along the z-axis. This is achieved by the transformations:

$$\begin{aligned} &\mathbf{r}_i \cdot \mathbf{k}_1 \to x_i, \quad \mathbf{r}_i \cdot \mathbf{k}_2 \to y_i, \quad \mathbf{r}_i \cdot \mathbf{k}_3 \to z_i \\ &\frac{d\mathbf{r}_i}{d\tau} \cdot \mathbf{k}_1 \to \dot{x}_i, \quad \frac{d\mathbf{r}_i}{d\tau} \cdot \mathbf{k}_2 \to \dot{y}_i, \quad \frac{d\mathbf{r}_i}{d\tau} \cdot \mathbf{k}_3 \to \dot{z}_i \end{aligned} \tag{10}$$

where

$$\mathbf{k}_1 = \frac{\mathbf{J} \times \mathbf{k}}{|\mathbf{J} \times \mathbf{k}|}, \quad \mathbf{k}_2 = \frac{\mathbf{J} \times (\mathbf{J} \times \mathbf{k})}{|\mathbf{J} \times (\mathbf{J} \times \mathbf{k})|}, \quad \mathbf{k}_3 = \frac{\mathbf{J}}{|\mathbf{J}|}$$

and

$$\mathbf{J} = \sum m_i \left(\mathbf{r}_i \times \frac{d\mathbf{r}_i}{d\tau}\right), \quad \mathbf{k} = (0, 0, 1).$$

Normally we will only be interested in coordinates, velocities and other physical quantities at certain times which are decided by external control. The following information may be obtained at any time:

(i) m_i, $\mathbf{r}_i$, $d\mathbf{r}_i/d\tau$, $\mathbf{F}_i$, E_i, $|\mathbf{J}_i|$ for each body.

Here $\mathbf{F}_i$ is the force, E_i the binding energy and $\mathbf{J}_i$ the angular momentum, all given per unit mass. The binding energy is defined by

$$E_i \equiv \Omega_i - T_i = \sum_{\substack{j=1 \\ j \neq i}}^{N} \frac{m_j}{[|\mathbf{r}_j - \mathbf{r}_i|^2 + \epsilon^2]^{1/2}} - \frac{1}{2}\left(\frac{d\mathbf{r}_i}{d\tau}\right)^2 \tag{11}$$

with Ω_i and T_i as potential and kinetic energy per unit mass, respectively.

(ii) $\tau, I_x, I_y, I_z, |\mathbf{J}|, \langle\omega_z\rangle, E, g.$

This is the main control line, giving the overall situation at time τ. I_x, I_y, I_z are the three components of the moment of inertia and $\langle\omega_z\rangle$ is the mean rotation given by

$$\langle\omega_z\rangle = \frac{|\mathbf{J}|}{I_z}. \tag{12}$$

The total energy of the system is defined by

$$E \equiv \Omega - T = \tfrac{1}{2} \sum_{\substack{i,j=1 \\ j\neq i}}^{N} \frac{m_i m_j}{[|\mathbf{r}_j - \mathbf{r}_i|^2 + \epsilon^2]^{1/2}} - \frac{1}{2} \sum_{i=1}^{N} m_i \left(\frac{d\mathbf{r}_i}{d\tau}\right)^2. \tag{13}$$

Thus E is not related to $\sum m_i E_i$ in any simple way because $\Omega = \frac{1}{2}\sum m_i \Omega_i$. Finally, g represents the virial theorem check

$$g = \frac{2T}{V}. \tag{14}$$

(iii) $\langle E_i\rangle$, $\langle|\mathbf{J}_i|\rangle$, $\langle r_i\rangle$, $\langle v_i^2\rangle$ for each group of equal mass, where v_i is the velocity of the ith body and $\langle\ \rangle$ denotes ordinary averaging. This enables us to compare average quantities for different masses.

3. *The initial condition.*—The main object of this paper is to study clusters with relatively large N. Hence only a few initial conditions can be tried and a restriction is therefore imposed on the generality of the results. The effects from variations in the initial condition will be damped out when the systems are integrated long enough, provided $g < 1$ which is the condition for a bound cluster. We are here concerned with models of physical systems, and integration times $\sim 10^{10}$ yrs are not really long enough for traces of the initial situation to vanish. A wide range of initial conditions cannot be studied when N is very large. We therefore examine two distinct possibilities:

(i) spherical clusters near equilibrium;

(ii) irregular clusters in contraction.

The possibility (i) does not by itself limit comparisons with actual physical models since it appears that many clusters have spherical shapes. Furthermore, it is not necessary to have a model for the way in which the clusters are formed since the initial situation may represent an arbitrary phase in their life history.

The simplest starting model would be to choose constant density, but this does not seem satisfactory on physical grounds. Even for young clusters one would expect to find a gradual decline in density with distance. Moreover, in the case of constant density encounter effects in the outer regions might lead to an overestimate in the number of bodies that are ejected into the halo. Instead, we choose a linear density function, viz.

$$\rho(r) = \rho(0)\left[1 - \frac{r}{R}\right] \tag{15}$$

where the cluster radius is R. The N bodies of total mass $M = \pi/3\,\rho(0)R^3$ are then distributed at random within 10 shells according to eqn. (15). In the case $N = 50$ we take 3 mass groups of relative masses 0·2, 0·8, and 2·7 consisting of 15, 25, and 10 members, respectively. In this model, therefore, more than half the total mass is contained in the heavy bodies. For the cluster $N = 100$, 4 different

groups are chosen with relative masses 0·25, 0·75, 1·50, 3·75, and with a membership of 40, 30, 20, 10 bodies, respectively. The mass ratios between heavy and light bodies are 13·5 and 15 in these models; this enables us to apply the results to actual galaxy clusters where such ratios are likely to exist. It proves simplest to use spherical coordinates, r, θ, ϕ for the actual distribution, the rectangular coordinates then follow immediately. Lastly, a check is made to avoid close neighbours.

The initial velocity distribution is chosen in such a way that for $g=0{\cdot}50$ no velocity shall be great enough to take a body outside $r=R$, provided the motions are due to a central force field only. This model of initial confinement will make it harder to provide a halo of bodies outside $r=R$ than if, say, a Maxwellian velocity distribution were chosen. The restrictions on the maximum permitted velocities are

$$\left.\begin{aligned} v^2_{\max}(r) &= v_c^2(r)+\dot{r}^2_{\max}(r) \\ |\dot{r}(r)| &\lesssim |\dot{r}_{\max}(r)| \end{aligned}\right\} \tag{16}$$

where $v_c(r)$ is the circular velocity at r arising from the mass distribution (15) and $\dot{r}_{\max}(r)$ is the radial velocity at r needed to reach the boundary $r=R$. This gives the criteria

$$\left.\begin{aligned} v^2_{\max}(r) &= \frac{GM}{R}\left[2-\left(\frac{r}{R}\right)^2\right], \\ \dot{r}^2_{\max}(r) &= \frac{2GM}{R}\left[1-2\left(\frac{r}{R}\right)^2+\left(\frac{r}{R}\right)^3\right]. \end{aligned}\right\} \tag{17}$$

We now randomize kinetic energy according to

$$v^2(r) = \frac{pq}{100}\, v^2_{\max}(r) \tag{18}$$

where pq is a random number. Put $\dot{x}=\gamma l$, $\dot{y}=\gamma m$, $\dot{z}=\gamma n$, where l, m, n are three random numbers. The scaling factor γ is then given by

$$\gamma^2 = \frac{v^2(r)}{l^2+m^2+n^2}. \tag{19}$$

Finally, a test on the radial velocity is performed according to (16) and (17); if the condition is not satisfied a new set of random numbers is tried. It turns out that this method of choosing velocities gives a r.m.s. value near to the value obtained from the virial theorem for the mass distribution (15). The application of (9) will therefore not change the velocities in such a way that eqns. (17) are violated, nor will in general the centre of mass correction be significant. The distribution procedure discussed above is used for both $N=50$ and $N=100$ and we take $g=0{\cdot}50$ in order to have stable systems.

The starting conditions for the irregular clusters will be discussed fully in Section 9.

4. *Relaxation time and crossing time.*—No method has been developed for the computation of the relaxation time; instead we will rely on relations between the time unit and the crossing time. Since we are dealing with clusters of galaxies

times $\sim 10^{10}$ yrs are of interest. From the knowledge of present-day values of galactic masses and cluster sizes one can then estimate the required values of the scaled time τ. The mean square velocity can be written in scaled units as

$$\langle v^2 \rangle = \frac{\kappa N}{r_0} \tag{20}$$

where r_0 is the initial scaled cluster radius and κ is a structural constant depending on the density distribution. Apart from fluctuations in the virial theorem check $\langle v^2 \rangle$ stays constant in time, hence (20) can be used with constant κ. For $N = 100$ we find $\kappa = 0{\cdot}71 \pm 0{\cdot}03$ when variations in g are included, and a similar value is found for $N = 50$ but with larger scatter. It will therefore suffice to use $\kappa \sim 0{\cdot}70$ throughout.

The crossing time, τ_{cr} is defined as the time taken for a body to move a distance $2r_0$ with r.m.s. velocity, hence from (20)

$$\tau_{cr} = \frac{2r_0^{3/2}}{(\kappa N)^{1/2}} \sim \frac{4{\cdot}8}{\sqrt{N}} \tag{21}$$

where the value $r_0 = 1{\cdot}60$ applies to linear density. The physical times corresponding to (21) will be approximately invariant as long as mass homology is considered since then $t_{cr} \propto \sqrt{N}\tau_{cr}$.

In defining the mean relaxation time, $\langle T_{E+} \rangle$, we follow Chandrasekhar (3) and write

$$\langle T_{E+} \rangle \sim \frac{\lambda}{[\langle v^2 \rangle]^{1/2}} \tag{22}$$

where the mean free path λ is given by

$$\frac{\lambda}{\langle r \rangle} = 0{\cdot}023 \frac{N}{\log_{10} N - 0{\cdot}56}. \tag{23}$$

In our notation $\langle r \rangle \sim 0{\cdot}7\, r_0$, hence elimination of λ and $\langle v^2 \rangle$ from (22) gives the mean relaxation time in scaled units:

$$\langle T_E \rangle \sim 0{\cdot}038 \frac{\sqrt{N}}{\log_{10} N - 0{\cdot}56}. \tag{24}$$

Thus for $N = 50$ and $N = 100$ we find $\langle T_E \rangle \sim 0{\cdot}24$ and $\sim 0{\cdot}27$ respectively, whereas the crossing times are $\sim 0{\cdot}70$ and $\sim 0{\cdot}48$. Eqn. (24) therefore indicates that there are about 4 mean relaxation times per scaled time unit for N in the range 50-100.

A standard cluster of galaxies is now defined in order that one may readily compare scaled values with physical ones. It will be convenient to make the time unit equivalent to 10^{10} yrs in the case when $N = 100$. Choosing a mean mass $10^{11} \odot$ eqn. (4 *a*) then gives $R \sim 560$ kpc for the total cluster radius. With mass and radius in units of $\odot$ and kpc the general form of eqn. (4 *a*) is

$$t\,(\text{yrs}) \sim 10^{10} \left(\frac{R}{560}\right)^{3/2} \left(\frac{10^{11}}{\langle M_i \rangle}\right)^{1/2} \tau. \tag{25}$$

We take the standard cluster $N = 50$ to be homologous to $N = 100$, viz. $R \propto N^{1/3}$ which gives a time unit corresponding to $\sim 7 \times 10^9$ yrs. Length units in the standard models are equivalent to ~ 350 kpc and ~ 250 kpc respectively and the velocity units are ~ 36 km sec^{-1} and ~ 26 km sec^{-1}.

5. *Structural evolution of spherical clusters.*—The detailed dynamical state of a cluster is determined by the distribution of mass and velocity. For an overall description, however, one can rely on the moment of inertia and the virial theorem check. Fig. 1 shows the plots of I for a time-scale in accordance with the standard clusters. (The cosmical expansion effects are discussed in the next section.) The changes in I are considerable and appear to be approximately linear. Initially, $\dot{I}=0$ but this still allows for the possibility $\ddot{I}\neq 0$. The early developments of I indicate that the initial conditions are fairly stable.

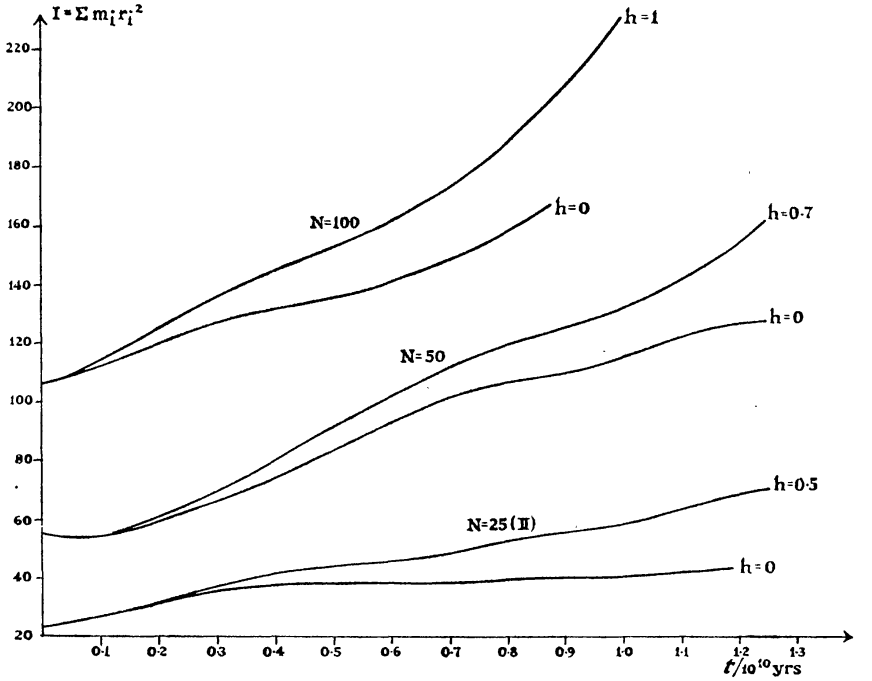

FIG. 1.—*Moment of inertia for $N=100$, 50, and 25 (II) with and without universal expansion. Units of time are based on the standard model $N=100$ and the homology relation $t=10^9N^{1/2}r$ yrs.*

Two processes of opposite nature are at work trying to change the moment of inertia:

(i) halo formation;

(ii) mass increase in the inner regions.

Both (i) and (ii) are due to the combined effects of close encounters and fluctuations in the general force field. When a close encounter takes place there is an energy exchange resulting in increased and decreased mean distances, respectively. Since it is generally the lighter bodies which are thrown outwards it is not clear that the moment of inertia for the two bodies combined will increase. It is shown in the Appendix that during a close encounter there is a net gain in the moment of inertia provided $\partial^2\Phi/\partial r^2>0$, which is also the condition for the density to decrease with distance. Hence it seems that I will tend to increase in clusters where encounter effects are important even if bodies do not escape to infinity.

Close encounters promote equipartition through the energy exchange. The general field fluctuations, however, tend to produce a Maxwellian velocity

distribution and the relative importance of this effect increases with N. The average fluctuation in the potential can be written as

$$\Delta\Phi \sim \frac{1}{\sqrt{N}} \frac{\kappa N}{r_0} \tag{26}$$

where $\kappa N/r_0$ is the potential corresponding to $\langle v^2 \rangle$. For the mean spatial separation between the bodies we write $d \sim 2r_0/N^{1/3}$. The number of very close encounters is small and we will therefore take the most efficient encounter distance as a fraction of d, say, fd. The ratio between the fluctuating field and the encounter field is then

$$\frac{\Delta\Phi}{1/fd} \sim 2\kappa f N^{1/6}. \tag{27}$$

A correction to (27) is needed if differences in mass are allowed for, but in any case it is clear that the general field fluctuations will dominate from a certain N, say, $N \sim N'$. This means that the effects of close encounters will be relatively unimportant for $N \gg N'$. The dynamical evolution of such clusters will be similar, and very little can be gained by increasing N any further. If we tentatively put $f \sim 1/3$, $\kappa \sim 0{\cdot}70$ then $N' \sim 90$, but clearly the result is very sensitive to the choice of f and κ. Only actual integrations of similar cases can therefore give a more reliable value for N'. The development towards equipartition is a very slow process. During the integration of the case $N = 100$, $h = 0$ only a factor $\lesssim 2$ is gained in the ratio between the kinetic energies for the mass groups $m = 0{\cdot}25$ and $m = 3{\cdot}75$, which initially have comparable mean velocities.

The central mass concentration does not go on increasing indefinitely, but is controlled by the process of mass depletion which takes place in the intermediary cluster region. The mean density within the initial radius declines with time and structural changes therefore proceed at a slower rate. The initial and final mass distributions for $N = 100$, $h = 0$ are shown in Fig. 2 *a*, where the mass within spherical shells of thickness $\Delta r = 0{\cdot}15$ is plotted.

Similar results for $N = 50$, $h = 0$ are shown in Fig. 2 *b*, in this case $\Delta r = 0{\cdot}20$. The zones of mass depletion show up well around $r \sim 1$. From Fig. 2 we find that for $N = 100 \sim 14$ per cent of the total mass is outside the initial sphere $r_0 = 1{\cdot}60$, while for $N = 50$ the halo fraction ~ 28 per cent. The clusters have therefore increased their volumes considerably, indicating an increase in the observational radius by ~ 50 per cent. Thus a cosmological effect would be present if the linear dimensions of similar near and distant clusters are compared.

The virial theorem check tells us about the rate of change in the moment of inertia. Even if $g = 0{\cdot}50$ initially there will be variations about this value. For a sufficiently long time, however, $\langle g \rangle = 0{\cdot}50$ when $h = 0$. Following Limber (4) let us denote the deviation of the virial theorem from unity by Λ, hence

$$\Lambda = 2g - 1. \tag{28}$$

$\Lambda = 0$ if all orbits are circular, whereas there is enough energy for all bodies to move to infinity when $\Lambda \gtrsim 1$. On the other hand, the smallest value is $\Lambda = -1$ and occurs if all bodies are at rest at the same time. If the mean mass is computed from the virial theorem on the assumption that $\ddot{I} = 0$, then Λ denotes the relative error. The variations in Λ may not exceed the observational errors for large clusters near equilibrium, but should be included in the total error estimates.

Results for the two spherical clusters are summarized in Table I together with the two smaller clusters discussed in the next section.

Dynamical effects on individual bodies are correlated to the mass, and a comparison of different masses may be instructive. The relative masses chosen for $N=100$ may tentatively be associated with four groups of galaxies; I: dwarf members; II: spirals; III: normal ellipticals; and IV: heavy ellipticals.

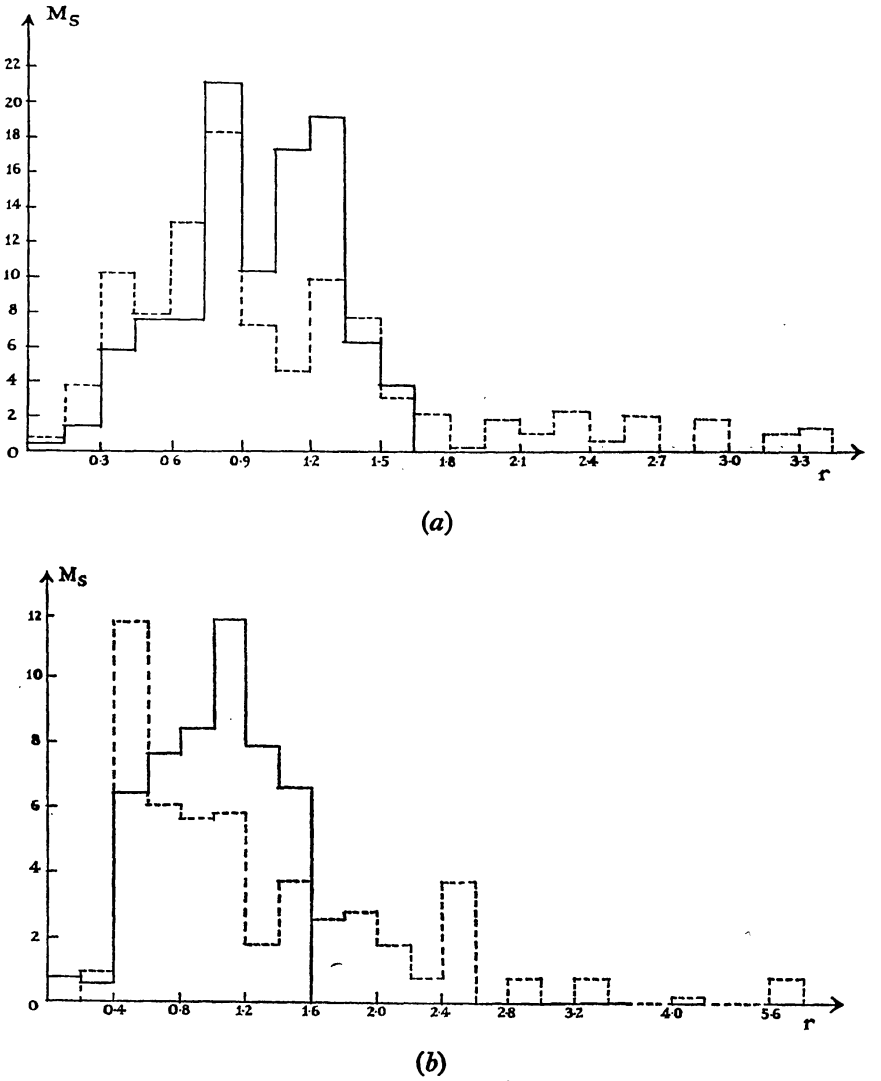

FIG. 2.—(*a*) *Mass within spherical shells of thickness* $\Delta r=0{\cdot}15$ *for* $N=100$, $h=0$.
———: $\tau=0$. – – – – –: $\tau=0{\cdot}87$.
(*b*) *Mass within spherical shells of thickness* $\Delta r=0{\cdot}20$ *for* $N=50$, $h=0$.
———: $\tau=0$. – – – – –: $\tau=1{\cdot}75$.

TABLE I

Departures from the virial theorem

	$h=0$		$h>0$	
N	Λ_{max}	Λ_{min}	Λ_{max}	Λ_{min}
100	+5 per cent	−5 per cent	+5 per cent	−7 per cent
50	12	15	18	18
25(I)	...	...	32	6
25(II)	23	15	54	16

Fig. 3 gives the mean radius for the different mass groups in the case $N=100$, $h=0$. The relative development is to some extent influenced by the initial condition and Fig. 3 should therefore be studied together with Fig. 4 which gives the mean binding energy per unit mass. The first and third mass groups are relatively strongly bound at $\tau=0$ compared to the neighbouring groups with higher mass. The situation is reversed at the end of the integrations and the changes in $\langle r_1 \rangle$ and $\langle r_4 \rangle$ are considerable.

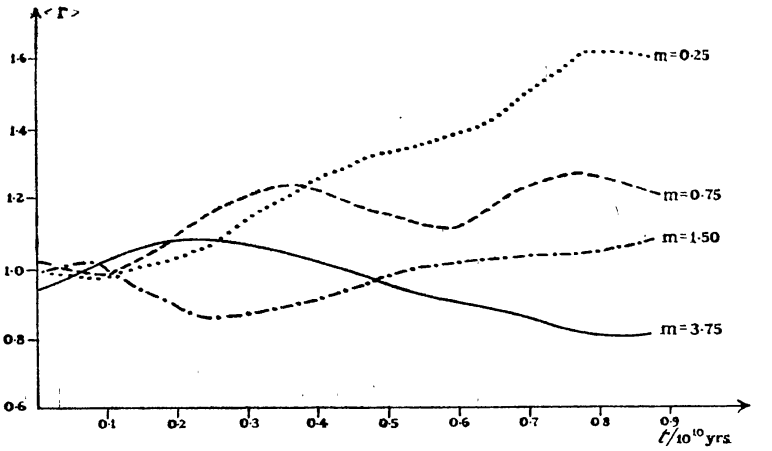

FIG. 3.—*Mean radius for different mass groups;* $N=100$, $h=0$.

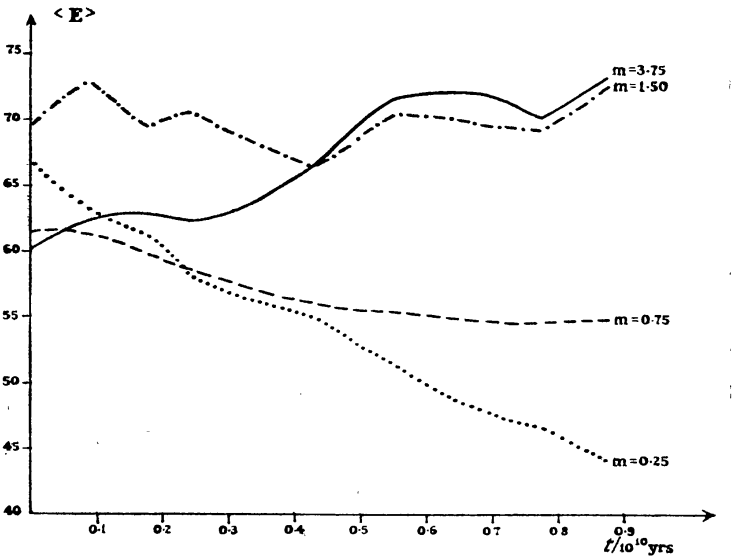

FIG. 4.—*Mean binding energy for different mass groups;* $N=100$, $h=0$.

TABLE II

Mean angular momentum per unit mass for different mass groups: $N=100$, $h=0$ *(in order of increasing mass)*

τ	$\langle\lvert J_1\rvert\rangle$	$\langle\lvert J_2\rvert\rangle$	$\langle\lvert J_3\rvert\rangle$	$\langle\lvert J_4\rvert\rangle$	τ	$\langle\lvert J_1\rvert\rangle$	$\langle\lvert J_2\rvert\rangle$	$\langle\lvert J_3\rvert\rangle$	$\langle\lvert J_4\rvert\rangle$
0·00	5·0	5·8	4·6	5·4	0·43	6·7	6·1	4·8	5·0
0·09	5·4	6·1	4·9	5·3	0·55	6·6	6·2	4·8	4·5
0·17	5·9	6·1	5·0	5·0	0·67	6·6	6·3	4·9	4·4
0·24	6·3	6·2	4·8	4·8	0·77	6·7	6·1	4·8	4·3
0·33	6·4	6·5	4·6	4·8	0·87	7·0	6·2	5·1	4·5

Mean angular momentum per unit mass is given in Table II. As can be expected from a random velocity distribution $\langle E_i \rangle$ and $\langle |\mathbf{J}_i| \rangle$ are anti-correlated. The reversal in relative value of $\langle |\mathbf{J}_i| \rangle$ for the two lightest and heaviest mass groups is shown very clearly, and again the effects are in opposite direction. From Table II and the knowledge of $\langle v^2 \rangle$ for each mass group we compare the mean radial velocity component $\langle v_r \rangle$ to one mean component in the tangential direction, $\langle v_t \rangle / \sqrt{2}$, where $\langle v_t \rangle = \langle |\mathbf{J}_i| \rangle / \langle r_i \rangle$ for all i of the same mass. The two different modes of velocity are compared at the beginning and end of the integrations for $N = 100$; a 5 per cent decrease in the velocities should be applied at $\tau = 0{\cdot}87$ if one wants a reduction to $g = 0{\cdot}50$. The results are given in Table III, and it appears that the mean transverse velocities are not significantly changed. The radial component on the other hand has increased markedly for the two light mass groups. The situation is complicated by the fact that for the 19 bodies outside $r = 2{\cdot}0$ ($m < 1$ for 16 of these) $\langle v_t \rangle / \sqrt{2} \sim \langle v_r \rangle \sim 2{\cdot}2$. Bodies in this region are about to turn round and move inwards again and v_r must become zero at a certain point, whereas this condition does not apply to v_t. We therefore conclude that the light bodies show a significant excess of radial velocities over the heavy ones in the main parts of the cluster.

TABLE III

Mean radial and tangential velocities for different masses: $N = 100$, $h = 0$

	$\tau = 0$		$\tau = 0{\cdot}87$	
m	$\langle v_r \rangle$	$\langle v_t \rangle / \sqrt{2}$	$\langle v_r \rangle$	$\langle v_t \rangle / \sqrt{2}$
0·25	3·8	3·6	6·0	3·1
0·75	4·1	4·0	5·8	3·6
1·50	3·7	3·3	4·2	3·4
3·75	3·8	4·0	3·4	3·9

The dynamical state of a cluster can also be described by the distribution of energy and angular momentum. Initially, the E_i, $|\mathbf{J}_i|$ distribution for $N = 100$ can be approximated to a linear relation where the relative mean spread in binding energy $\sim \pm 10$ per cent. This distribution reflects the way in which the initial condition is chosen. During the integrations each body suffers changes in E_i and $\mathbf{J}_i$, again due to the combined effects of close encounters and general field fluctuations. The final distribution shows a much wider spread in energy, but still no body has sufficient energy to escape the cluster by itself. The total effect is one of diffusion in the energy coordinate, but one should visualize the individual bodies to move about in the E_i, $|\mathbf{J}_i|$ plane.

From the knowledge of E_i and T_i for each body it is possible to evaluate the relaxation time directly. For a system not in a steady state the random walk method of estimating $\sum \Delta E_i^2 / N \langle T_i^2 \rangle$ is not a satisfactory way of evaluating the relaxation time. In our cases the mean changes in energy are systematic, at least for light and heavy masses. Limber (**12**) has discussed more fully the relaxation of systems that are time-dependent and we shall adopt his expression for the mean relaxation time for a group of equal mass:

$$\frac{\langle |\Delta E_i| \rangle}{\langle T_i \rangle} = \frac{d\tau}{\langle T_E' \rangle} \tag{29}$$

where we take $\langle T_i \rangle$ to be averaged over the time $d\tau$. Two points are worth making in connection with the use of (29):

(i) bodies in close encounters at the time $d\tau$ may have a larger value of ΔE than at a later time;

(ii) some bodies experience random changes in energy rather than systematic ones.

The effects of (i) and (ii) will tend to cancel out, *provided the interval $d\tau$ is chosen suitably.*

Computed mean relaxation times for different mass groups: $N=50$ and $N=100$

m	$d\tau$	$\langle T_E' \rangle$	m	$d\tau$	$\langle T_E' \rangle$
0·2	0·46	0·58	0·25	0·43	0·69
0·8	0·46	0·80	0·75	0·43	0·86
2·7	0·46	0·55	1·50	0·43	0·72
			3·75	0·43	0·77

The values of $\langle T_E' \rangle$ are 2-3 times larger than those for $\langle T_E \rangle$ as given by (24). The mean relaxation times therefore appear to be in better agreement with those computed by King (**13**) on the basis of centrally concentrated models. A direct comparison of $\langle T_E' \rangle$ for different masses is hardly relevant because of the different initial values of the mean binding energies. As time goes on the mean distances for the two lighter mass groups will increase and this will certainly slow down any further changes in the binding energies, whereas the heavy masses will become more concentrated towards the centre and consequently the process of their equipartition will be speeded up. The results of the mean relaxation times should be treated as tentative values which may be compared to the actual integration times. In the case $N=50$ the total integration time would therefore correspond to $\lesssim 3\langle T_E' \rangle$ whereas for $N=100$ about one mean relaxation time has been studied.

The final velocity distributions for $N=50$ and $N=100$ show a surprisingly close agreement with a normalized Maxwellian when all masses are included. Some of the high-velocity bodies could be due to close encounters rather than to low binding energies, but the probability for this to happen is too small to be significant.

Chandrasekhar (**5**) has discussed the effect of dynamical friction and shown that there is a tendency for bodies to be slowed down in their motion. This means that a longer time will be needed for high velocities to be built up. Hence clusters will lose less members than is indicated by calculations with a Maxwellian velocity distribution, where the expected loss $\sim 0{\cdot}007\,N$ per relaxation time. When the derived mean relaxation times are used we would therefore expect about one escaper in both cases, whereas none is found. The absence of escapers need not be the result of dynamical friction, however, but may instead be due to the initial energy cut-off. A final conclusion on the escape rate must therefore wait until the further interaction of low-energy bodies has been studied.

6. *Universal expansion.*—We will now make a comparison between the two cosmological alternatives $h=0$ and $h>0$. The scaled Hubble's constant is given by eqn. (4*b*). We take $H^{-1}=10^{10}$ yrs; the standard models then give $h=1$ for $N=100$ and $h=0{\cdot}7$ for $N=50$. From the equation of motion (3)

$$E_i \equiv \Omega_i - T_i = E_i(0) + \tfrac{1}{2}h^2 r_i^{\,2}(0) - \tfrac{1}{2}h^2 r_i^{\,2} \qquad (30a)$$

where the binding energy is defined in the same way as before (cf. eqn. 11) and $E_i(0)$ is the initial value of E_i. The total energy is then

$$E \equiv \tfrac{1}{2}\sum_{i=1}^{N} m_i \Omega_i - \sum_{i=1}^{N} m_i T_i = E_0 - \tfrac{1}{2}h^2 \Delta I \tag{30b}$$

where ΔI is the change in the moment of inertia. The term $\frac{1}{2}h^2\Delta I$ represents the amount of energy pumped into the system by the expansion and may be compared directly to the actual values of $\Delta E = E - E_0$, provided integration errors are small. The moments of inertia for $N = 100$, $N = 50$, and $N = 25$(II) are drawn in Fig. 1 where they can be compared to the cases $h = 0$.

TABLE IV

Expansion effects on total energy and r.m.s. distance

N	τ	$-\Delta E/E_0$	$\Delta E_{max}/E_0$	$\frac{1}{2}h^2\Delta I/E_0$	$r_w(h=0)$	$r_w(h>0)$
100	0·87	2·6 per cent	0·4 per cent	2·9 per cent	1·28	1·42
50	1·74	8·5	$\gtrsim$3·0	5·3	1·60	1·80
25(I)	2·33	14·7	$\sim$0·3	14·7	...	2·66
25(II)	2·29	3·9	$<$0·2	4·0	1·30	1·61

Table IV summarizes the results of (30*b*). Actual deviations are given in column 3 and column 4 contains the maximum integration errors for the cases $h = 0$. The predicted energy decreases in column 5 are in good agreement with the actual ones when integration errors are allowed for. Data for the two clusters $N = 25$ (I) and (II) are selected from the clusters $N = 100$ and $N = 50$, respectively and are integrated to a greater accuracy than for the large clusters. The last two columns in Table IV will be used in connection with eqn. (33).

The contribution from universal expansion to the term $\sum \mathbf{r}_i \cdot (m_i\, d^2\mathbf{r}_i/d\tau^2)$ in the virial theorem is $h^2 \sum m_i r_i^2$. The virial theorem should therefore be written in the form

$$\tfrac{1}{2}\ddot{I} = 2T - \tfrac{1}{2}V + h^2 I. \tag{31}$$

Since $g = 2T/V$ is computed and $2T = N\langle v^2\rangle$ we also know $\ddot{I}$, viz.

$$\ddot{I} = N\langle v^2\rangle[1 - 2/g] + 2h^2 I. \tag{32}$$

Thus, in the case where expansion is included we may have that $\ddot{I} > 0$ even for $g < 0{\cdot}50$. The integrations where h is included give $\langle g\rangle \sim 0{\cdot}50$, and the results in Table I show that the departures from this value are again relatively small for large N. When Λ is small, therefore, the terms $\ddot{I}$ and $2h^2 I$ will tend to cancel each other out. This means that the normal procedure of mass determination, $2T \sim \frac{1}{2}V$, will lead to the same results as (31) apart from the Λ-variations.

The weighted r.m.s. distance is defined as

$$r_w = \left[\frac{1}{N}\sum m_i r_i^2\right]^{1/2}. \tag{33}$$

Initially, $r_w \sim 1$ on account of the scaling conditions $\langle m_i\rangle = \langle r_i\rangle = 1$. The final values of r_w are given in Table IV; column 6 contains the values when $h = 0$ and the last column gives the results when expansion is included. The expansion force $h^2\mathbf{r}$ is derivable from the potential $-\frac{1}{2}h^2 r^2$ and the energy decrease caused by the expansion can therefore not be predicted in advance.

Bodies belonging to the halo region of a cluster experience an inward force $\sim N/r^2$. This force is balanced by the expansion force $h^2 r$ at a distance

$$r_h \sim \left(\frac{N}{h^2}\right)^{1/3}. \tag{34}$$

This means that any cluster galaxy outside this distance is dominated by the expansion force and will be lost by the cluster even if the binding energy w.r. to infinity may still be positive. All bodies satisfying $r \gtrsim r_h$ should therefore be counted as ejected cluster members. Clearly the dynamical effect of these on the rest of the cluster will be small; their contribution to the computed quantities is therefore included, especially since in our cases most of the escaping bodies have not had time to move very far from the main cluster.

Secondly, bodies with large central distances but still within $r \sim r_h$ may in certain cases be included in the number of ejected bodies, even if they would need some time to leave the cluster region. Such cases will be counted, provided the following conditions are satisfied:

(i) $\dot{r} > 0$; e.g. the motion is actually outwards;

(ii) the energy w.r. to the sphere of influence is $\lesssim 0$, viz.

$$E_i - \Phi_h \lesssim 0$$

where $\Phi_h \sim N/r_h$ is the potential at $r \sim r_h$;

(iii) no more encounters are likely to take place.

The bodies in question will eventually be lost by the cluster if the above conditions are fulfilled, even without any further action by the expansion force.

TABLE V

Ejection of cluster members when the expansion force is present (the values of scaled time are approximately homologous)

N	h	τ	N_1	N_2	$(N_1+N_2)/N$	$\Sigma m/N$
100	1·0	1·00	3	8	11 per cent	6 per cent
50	0·7	1·48	2	4	12	6
25(I)	0·5	2·10	3	6	36	17
25(II)	0·5	2·04	2	3	25	10

The relevant data are given in Table V at approximately homologous times. The total number of ejected bodies is made up of the two contributions discussed above; N_1 is the number for which $r \gtrsim r_h$, and there are N_2 bodies satisfying the conditions (i)–(iii). In all there are 31 escapers, 6 of which have $E_i < 0$. Of the latter, 2 bodies in the cases $N = 25$ become negatively bound through dynamical interactions. If the escaping bodies are analysed according to mass we find 18 with masses 0·20–0·25, 11 with masses 0·75–0·92, and 2 with $m = 1·50$. The total number of bodies in the three mass groups is 75, 72, and 27, respectively. The reason why an even greater number of the lightest bodies is not escaping is probably because the velocity distribution is still far from being in equipartition but one should also remember that initially (for $N = 50$ and $N = 100$) these are quite well bound.

The initial data for the cases $N=25$ are not checked in the same manner as for the other clusters and there is a possibility that some bodies have large velocities at $\tau=0$. It turns out that among the escapers only one body in each case is relatively lightly bound, the others having average binding energies. It seems, therefore, that nearly all bodies included in Table V have been ejected as the result of the combined action of close encounters and expansion force. The results indicate that small systems may lose a greater proportion of their members than medium-sized ones. The mean free path increases with N and the importance of individual encounters will therefore be larger for small clusters. Hence a halo population is formed more quickly and this allows the expansion force to be effective during a longer time.

The process of increasing the central mass concentration does not appear to be affected by cosmic expansion for $N=50$, but this may well be due to fluctuations. Towards the end of the integrations of the case $N=100$, $h=1$ in the mean ~ 18 per cent of the mass lies within a radius $r=0{\cdot}60$, whereas for $h=0$ the average amount ~ 23 per cent. The cases $N=25$ (I) and (II), $h=0{\cdot}5$ have a mean mass concentration $\gtrsim 30$ per cent within the same volume and this shows that the small clusters have achieved a high degree of relaxation.

Only one value for the scaled Hubble's constant is tried in each case. If one wants to consider the effects of expansion on a different model the ratio t/τ will change according to eqn. (25) and, consequently h should take a different value for the same H. Specifically, a smaller value for the time unit would lead to a smaller h. The action of the expansion depends on the time average of the product $h^2\langle r_i\rangle\tau$. In order to compare results at the same physical times $h\tau=$ constant and a larger value of τ would be needed, hence the expansion effect would only decrease linearly with h. (The larger value of r_h demanded by (34) would be compensated by a greater halo formation.)

Lastly it should be pointed out that the effects of the force $h^2\mathbf{r}$ might be similar to that of tidal action, which is essentially in one dimension. Furthermore, in cosmologies where there is no expansion force tidal effects will still be present, especially if there is second-order clustering.

7. *Close encounters.*—The cluster members move about at random and there will be a certain number of encounters where the separation is comparable to the radius of a galaxy. Clearly these events will have dynamical importance provided they are numerous enough. Apart from the dynamical effect of energy exchange, two colliding galaxies may also interact physically. Observations of the relative distribution of galaxy types give different results for cluster members and field galaxies, the main difference being the large number of SO galaxies and heavy ellipticals in large clusters. Baade and Spitzer (**6**) have suggested that collisions between galaxies cause interstellar matter to be swept out while the stellar component is not appreciably disturbed.

The number of two-body encounters in a group of randomly moving objects can be estimated by

$$N_d \sim \frac{3\sqrt{2}}{4}\,\frac{vN^2a^2}{{r_0}^3}\,\tau \tag{35}$$

where v is the mean space velocity and a is the encounter parameter. Since the computer is not programmed to count N_d we must rely on visual inspection of the

positions printed after each step. Table VI contains the results of counted and predicted values of two-body encounters for two values of the parameter a. The scaled cluster radius $r_0 = 1{\cdot}60$, and $v \sim 4{\cdot}5$ and $\sim 6{\cdot}5$, respectively, for $N = 50$ and $N = 100$. In both cases the smaller value of a is equal to the value of ϵ; these encounters can therefore be taken to represent collisions. Eqn. (35) predicts a smaller value for N_d than is actually found when $N = 100$, this may indicate that the contribution from the inner regions becomes more important in large clusters. Furthermore, there is a relative deficiency of encounters for the larger impact parameters but this is a reflection of the difficulty of detection.

TABLE VI

The number of actual and predicted close encounters

N	τ	a	N_d(actual)	N_d(predicted)	a	N_d(actual)	N_d(predicted)
100	0·87	0·03	27	13	0·06	60	52
50	1·75	0·04	7	8	0·10	21	50

Baade and Spitzer's work deals with the large Coma cluster ($N \sim 800$) and the assumption of nearly radial orbits is used. On the basis of a r.m.s. velocity $\sim 1700\,\mathrm{km\,sec^{-1}}$ the authors estimate that during 3×10^9 yrs galaxies passing within 10′ ($\sim 0{\cdot}10\,r_0$) of the cluster centre experience ~ 20 and ~ 140 collisions, respectively, for $a = 4\,\mathrm{kpc}$ and $a = 10\,\mathrm{kpc}$. As the 1950 value for Hubble's constant is used there is a correction factor ~ 5 in all linear distances. Thus, if we use an uncorrected value ~ 140 collisions and a time $\sim 10^{10}$ yrs the corrections indicate $\lesssim 4$ collisions per galaxy. The corresponding number of collisions in Table VI is $2N_d \sim 54$ and it should be increased to about 60 to make a direct comparison ($\xi \sim 10\,\mathrm{kpc}$). Since this refers to the whole cluster we conclude that the effect of collisions in the Coma cluster may well be 5 times as effective as for the case $N = 100$. The efficiency of the process whereby interstellar matter is swept out of galaxies by collisions must therefore be quite high if the effects shall be significant for medium-sized clusters, and this would appear to justify the assumption of constant mass.

8. *Binary formation and stability.*—The number of close pairs observed in clusters of galaxies is larger than would be expected if the galaxies were distributed at random. From counts in regions of the Coma and Virgo clusters, Page (7) estimates that physical pairs form about 20 per cent of the optical pairs down to $18^{\mathrm{m}}{\cdot}5$.

There are several ways in which pairs may be formed:

(i) dynamical formation due to many-body encounters;

(ii) two condensations that are formed in the same region with small relative velocities at the time when they become discrete will start moving round each other in closed orbits;

(iii) fragmentation of a single galaxy.

The two first possibilities will be examined in the present paper with special regard to the dynamical stability.

Two bodies of masses m_1 and m_2 at a distance r_{12} are said to be bound if the relative energy is positive. Thus

$$E_{\mathrm{rel}} = \frac{m_1 + m_2}{[r_{12}^2 + \epsilon^2]^{1/2}} - \tfrac{1}{2} v_{\mathrm{rel}}^2 > 0 \qquad (36)$$

where v_{rel} is the relative velocity of the bodies. This relation should only be used when r_{12} is less than the mean spatial separation and there are no other close bodies; that is, when the tidal effect from the other bodies can be ignored. The criterion $r_{12} \lesssim 3(A_1 + A_2)$ for the separation of binaries is used by Page in the above mentioned search for double systems; A_1 and A_2 being the linear dimensions of the components. If we take $A_1 = A_2 = 2\epsilon$, then $r_{12} \lesssim 12\epsilon$ in our notation.

We now treat the possibilities (i) and (ii) separately and then attempt a relative comparison.

It is mentioned in Section 3 that a check is made in order to prevent close bodies initially. One would expect this to exclude possible stable binaries at $\tau = 0$, but integrations show that in the case $N = 100$ there are in all 3 double systems. In Table VII data are given for the three initial pairs *a*, *b*, *c*, both for $h = 0$ and $h = 1$. All pairs involve a heavy body of which there are only 10. The results show that it may be possible for binaries to remain stable for a time $\sim 10^{10}$ yrs on the standard model, even if the initial pairs are not very close. Maximum separation during the stable periods $\sim 0{\cdot}60$ which would correspond to ~ 200 kpc on the standard model. This means that even quite open pairs may survive the disruptive effects of the other bodies. Pair *b* forms a close pair at the end of the integration ($h = 1$) and it is clear that the binding has become stronger by dynamical interaction.

TABLE VII

Dynamical stability of initial pairs ($N = 100$)

		$h=0$				$h=1$			
Pair	m_1+m_2	τ	r_{12}	E_{rel}	Remarks	τ	r_{12}	E_{rel}	Remarks
a	5·25	0·00	0·35	12		0·51	0·39	12	
		0·51	0·13	(8)	Disrupting	0·60	0·36	...	Disrupting
b	5·25	0·00	0·41	(3·6)		0·36	0·05	20	
		0·67	0·09	16		0·60	0·10	28	
		0·77	0·41	(7)	Disrupting	1·00	0·13	28	Stable pair
c	4·00	0·00	0·35	(0)		0·24	0·62	...	Large separation
		0·20	0·63	(2)	Large separation	0·79	0·05	13	
		0·51	0·23	4		0·87	0·19	16	See Table VIII
		0·55	0·12	−2	Disrupting	1·00	0·28	(10)	3-body interaction

The computer programme is written in such a way that data for any number of bodies may be included after the initial adjustments have been performed. The spherical cluster $N = 50$ is provided with 6 initial close binaries and the extra mass is partly compensated for by using $g = 0{\cdot}60$ in the scaling of the velocities. All possible combinations of the masses $m = 2{\cdot}7$, 0·8, and 0·2 are included and the initial velocities of the components are such that the undisturbed orbits would give a semi-major axis $\sim 0{\cdot}16$ and largest separation $\sim 0{\cdot}20$. Furthermore, the centres of mass of the binaries have arbitrary velocities w.r. to the cluster centre. The integration is terminated at $\tau \sim 0{\cdot}37$, but even after this relatively short time only 2 of the initial pairs remain bound. During this period the moment of inertia decreases by ~ 20 per cent. The pairs are therefore more exposed to encounters than for normal evolution. The stable pairs at $\tau = 0{\cdot}37$ have combined masses 5·4 and 2·9, whereas 3 of the disrupted binaries are lighter. From these results we may conclude that light binaries in clusters will have relatively short life-times, even if the mean separation is small.

The problem of dynamical formation of binaries and higher-order systems from a set of freely moving bodies has been studied statistically (**8**). Here we will only mention a few factors relevant to the problem and then discuss the findings.

(i) *The importance of the general field.*

As N increases the general force field becomes more important in comparison to individual encounters. Since also the r.m.s. velocity is greater in large clusters one would expect the relative formation rate to decrease with N.

(ii) *The relative mass distribution.*

A condition on the third body in a successful binary formation is that it must be heavy enough to carry away the excess energy. Conditions are therefore best for equal masses.

(iii) *The velocity distribution.*

The central regions of a cluster may contain a relatively large proportion of low-velocity bodies. Centrally concentrated binaries could then be formed at a much higher rate than for average conditions, but the expected life-times would also be shorter.

A search for stable pairs has been carried out but due to the work involved one can only hope to find those with long life-times. Table VIII gives the result for $N = 100$, $h = 1$ and should be studied in connection with Table VII because 2 of the initial pairs are involved. Around $\tau \sim 0{\cdot}60$ pair a loses its light companion but recaptures another body of the same mass in a 5-body encounter. For a stable binary to become disrupted, one or more bodies nearby must give up kinetic energy. It is then possible that a disturbing body may be captured by the dominating companion as in the case above (" particle exchange "). As for pair c' this may be a triple system involving the initial pair c. Finally, the last pair is formed quite early and the binding is greatly increased at a later time.

TABLE VIII

Dynamical formation of pairs, $N = 100$, $h = 1$

Pair	m_1+m_2	τ	r_{12}	$E_{\rm rel}$	Remarks
a'	5·25	0·60	0·21	(−2)	Pair a in 5-body encounter.
		0·66	0·34	11	Formation of pairs a' and d.
		1·00	0·29	14	Well bound pair.
c'	7·50	0·87	0·46	(6)	Pair c still bound.
		0·96	0·09	13	Pair c is wide.
		1·00	0·27	(20)	Pair c have comparable distance.
d	3·00	0·66	0·04	17	Formation through interaction with a.
		0·74	0·14	18	
		0·96	0·22	(4)	The pair is disrupting.
e	5·25	0·44	0·43	(5)	Tidal effect may be large.
		0·51	0·19	5	
		0·60	...	...	Several close encounters.
		1·00	0·10	28	The pair is very stable ($r \sim 1{\cdot}3$).

Kepler's third law for the relative period of revolution can be written as

$$\tau_k^2 \approx \frac{4\pi^2(\langle r_{12}\epsilon^2\rangle + \epsilon^2)^{3/2}}{m_1+m_2}. \qquad (37)$$

Thus for $(\langle r_{12}^2 \rangle)^{1/2} \sim 10\epsilon = 0{\cdot}30$ and $m_1 + m_2 = 5{\cdot}25$, say, $\tau_k \sim 0{\cdot}45$. This rather long period should be kept in mind when examining open pairs.

The conclusions to be drawn from the data presented above must necessarily be tentative since only a relatively small number of pairs have been investigated. The case $N = 100$ gives several pairs with very long life-times. The binding energy for light pairs is relatively small, even when in close orbits. This might explain the apparent absence of light pairs formed dynamically; e.g. the expected life-times are small. On the basis of the results we conclude that only a small binary formation rate is required to ensure that old clusters would have as many stable double systems as it appears from observations. It seems likely that a proportion of the observed pairs have remained stable since the time when the galaxies were formed, especially in systems with large N where the general field tend to shield the disruptive effects due to encounters. Furthermore, the dynamical origin of very close pairs cannot be ruled out as shown by the example of pair *e* in Table VIII.

9. *Irregular clusters.*—The clusters that have been discussed so far have all nearly stable initial conditions, as well as roughly spherical shapes. Many spherical systems are observed but there is also a large number of irregular clusters, especially small ones (**9**). All irregular systems will change their structure on a fairly short time-scale and therefore lose traces of the initial conditions. But as the future development is determined by the starting conditions it is clear that these may be important. No satisfactory theory for the formation of galaxy clusters has yet been developed and one is therefore left to construct initial situations in an arbitrary way. If one takes the view that all clusters of galaxies have nearly the same age one is excluded from observational material altogether. Thus not even the results of present-day sizes and population numbers can safely be used to form typical starting conditions.

At the present time it is argued with stronger force that there exist clusters of galaxies that are dynamically unstable (expanding) and that this limits their past history to 10^8–10^9 yrs. Such conclusions are based upon use of the virial theorem, which gives a lower limit to the total mass when stability is assumed. On the basis of the discrepancy between mean galactic masses from this method as compared to the smaller masses obtained from studies of internal motions and double galaxies it is then concluded that this means instability and that therefore such clusters are disrupting. These results rest primarily on the assumption that the amount of dark matter in clusters is negligible. The evidence for this is not conclusive and we will therefore not consider expanding clusters in the present paper.

The large Hercules cluster is a particularly interesting irregular cluster. This system appears to have its main mass concentrated in a V-shape in space and consists of about 170 objects (**10**). It seems unlikely that such an irregular shape can be maintained for any long period of time or be the result of a chance configuration during a long life-time. One could therefore argue that the Hercules cluster is not very old and this would have cosmological implications.

Two different models with $N = 50$ are integrated in order that one may get an idea of the possible changes that irregular mass distributions can undergo. A V-shaped system with a halo population is taken to represent a Hercules-type cluster, the relative size is drawn in Fig. 5 in two dimensions. The x-coordinates are assigned at random, with $|x| \lesssim 0{\cdot}20$ for bodies in the V and $|x| \lesssim 0{\cdot}80$ for the halo objects, thus making the cluster rather flattened in the x-direction. Masses

are evenly distributed between $m=0{\cdot}50$ and $m=1{\cdot}50$ and are initially without velocities. The bodies will therefore start moving radially towards the centre of mass.

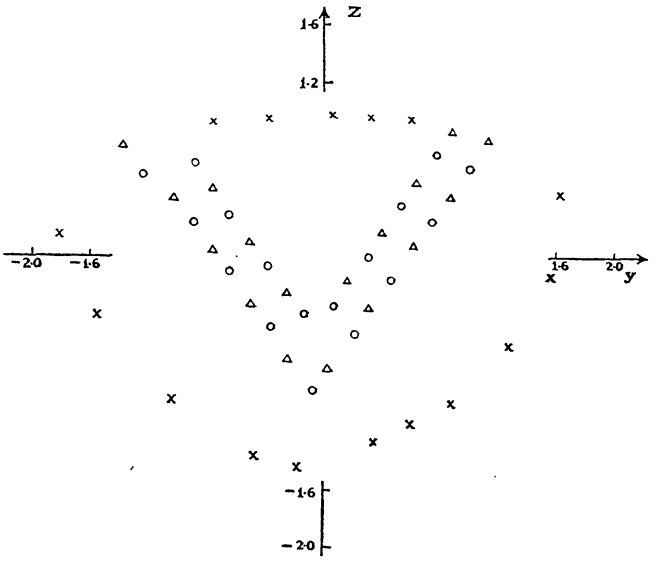

FIG. 5.—*Initial distribution in the yz-plane of V-shaped cluster with halo;* $N=50$, Δ: $m=1{\cdot}50$, o: $m=0{\cdot}50$, $\times$: *halo bodies.*

The initial situation will not be restored for two reasons (even for symmetrical clusters, excepting constant density):

(i) the times for complete oscillations are different;

(ii) most bodies experience close encounters during the contraction and this produces angular momenta of opposite signs.

Some of the radial kinetic energy is therefore converted into transversal velocities so that most of the bodies will have smaller central distances once the initial contraction and the following expansion has taken place. Fig. 6 shows the general contraction and expansion as measured by the moment of inertia. The apparent minimum is at $\tau\sim0{\cdot}30$ when $r_w\sim0{\cdot}50$. Mean distances for light and heavy masses are actually $\sim0{\cdot}41$ and $\sim0{\cdot}42$, respectively. When the 16 halo objects are omitted we find that the minimum contraction occurs at $\tau\sim0{\cdot}24$ and the mean distances are then $\sim0{\cdot}22$ and $\sim0{\cdot}21$. For the standard model $N=50$ the phase of overall contraction would correspond to $\sim2{\cdot}1\times10^9$ yrs and the contraction time for the V by itself $\sim1{\cdot}7\times10^9$ yrs. This relatively long time is partly due to the time it takes for the velocities to build up (half-value for velocities is reached around $\tau\sim0{\cdot}10$).

Initially $I_x\sim2I_y$, with I_z somewhat larger than I_y. The relation $I_x\sim2I_y$ is satisfied up to $\tau\sim0{\cdot}55$ while I_z increases more slowly than I_y and $I_z\sim I_y$ at $\tau\sim0{\cdot}63$. The fact that I_x is nearly twice as large as the two other components of I during most of the time shows that the system retains its degree of flattening during the initial contraction and following expansion. The structural changes of the cluster may be studied in the yz-plane because the x-coordinates are quite small for most bodies. The situations at $\tau\sim0{\cdot}28$, $0{\cdot}54$ and $0{\cdot}80$ are mapped in Fig. 7. Heavy bodies from the original V-shaped distribution are concentrated towards the central region where they move in a strong force field. At $\tau\sim0{\cdot}80$ there are

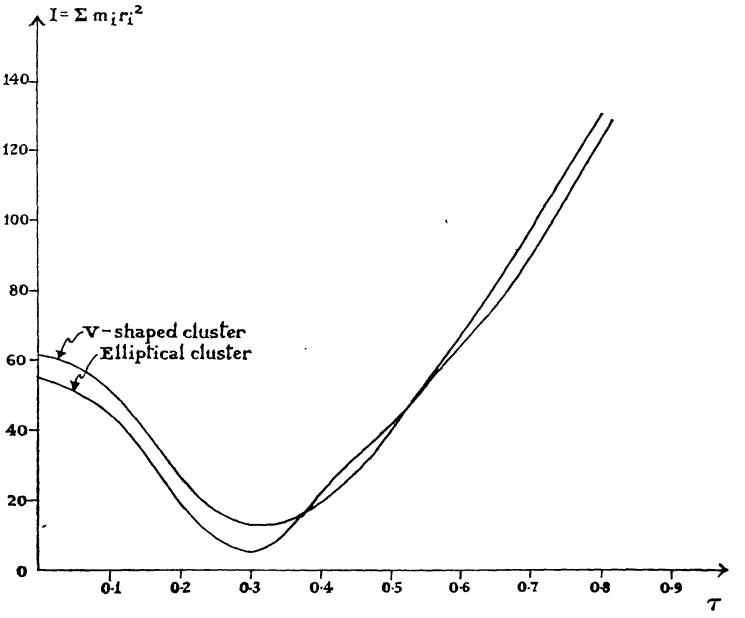

FIG. 6.—*Moment of inertia for two initially contracting irregular clusters; $N=50$ (units of scaled time).*

22 bodies within $r=0{\cdot}40$, 13 of which have $|\dot{x}|>3{\cdot}0$ as compared to the r.m.s. velocity $\sim 6{\cdot}4$. Thus it is to be expected that oscillations in the x-direction will finally make the system appear more regular. The large number of bodies to be found at any time within the sphere $r=0{\cdot}40$ indicates that the compact central region is fairly stable, in spite of the high velocities and strong force field.

In the second model of an irregular cluster 50 bodies are evenly distributed within an elliptical contour in the yz-plane. The x-coordinates are again chosen at random, with a maximum value equal to the minor axis in the plane. This time all the bodies are given small velocities chosen at random as so to avoid initial parallel orbits which may cause very close encounters. Since $\langle v^2\rangle \sim 0{\cdot}50$, however, the radial velocity component very soon dominates. The moment of inertia is shown in Fig. 6. By comparing with the previous case one sees that the minimum contraction for the systems as a whole is reached at approximately equal times, but the elliptical cluster has a smaller value for I. This is due to the phase lag between the halo population and the more concentrated V-distribution. At minimum $r_w \sim 0{\cdot}30$ and mean distances are $\sim 0{\cdot}29$ and $\sim 0{\cdot}27$ respectively for $m=0{\cdot}50$ and $m=1{\cdot}50$. In both cases the three moments of inertia are at a minimum within an interval $\Delta\tau \lesssim 0{\cdot}03$ which shows that the contraction proceeds at the same rate in all directions. In the case of the elliptical cluster $I_y \sim 2I_x$ nearly all the time, with I_z having intermediate values. (The orientation of the coordinate system is arbitrary in this case.) At the end of the integrations there are 3 bodies in each case with enough energy to escape from the clusters. There are also examples of bodies with $E_i<0$ giving up the free energy to become bound again; the importance of this will be discussed in the next section.

Unfortunately, there is a sudden change in the total energy around $\tau \sim 0{\cdot}64$; during an interval $\Delta\tau < 0{\cdot}03$ the change amounted to a relative decrease ~ 17 per cent, whereas the total change until then ~ 12 per cent decrease. This large decrease is mainly caused by a poor integration of a many-body encounter and the subsequent results are therefore uncertain.

At $\tau = 0$ only 5 bodies are within the sphere $r = 0{\cdot}40$ but at $\tau \sim 0{\cdot}59$ when the moment of inertia has again exceeded the initial value there are 21 bodies within this volume. In spite of the errors introduced around $\tau \sim 0{\cdot}64$ we may still examine the central sub-system. (The energy decrease probably means an erroneous loss of one or more bodies from the inner regions, hence the stability at later times is likely to be underestimated.) At $\tau \sim 1{\cdot}13$ there are 18 bodies within $r = 0{\cdot}40$, 13 of which have predominantly tangential velocities ($v_r < v_t/\sqrt{2}$). On the standard model $N = 50$ this value of τ would correspond to a time $\sim 8 \times 10^9$ yrs. It therefore appears that compact sub-clusters can remain stable for long periods of time.

An additional parameter concerning the stability is the binding energy. The mean binding energy of the bodies increases as the result of the formation of the sub-system. For example, initially, the elliptical cluster has $\langle E_i \rangle \sim 45$ and 43,

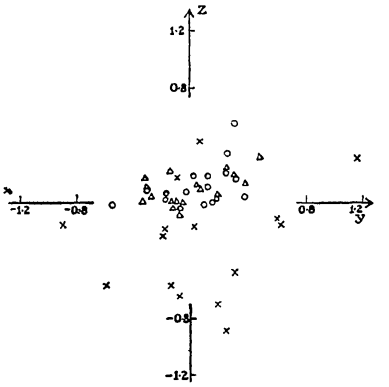

(*a*) $\tau = 0{\cdot}28$ (*Near minimum contraction*).

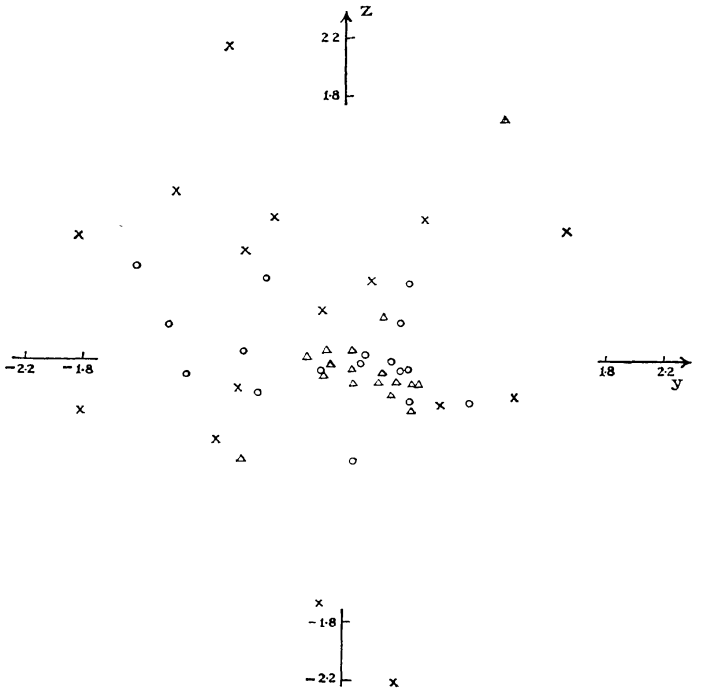

(*b*) $\tau = 0{\cdot}54$.

FIG. 7.—*Structural developments in the yz-plane of V-shaped cluster with halo.*

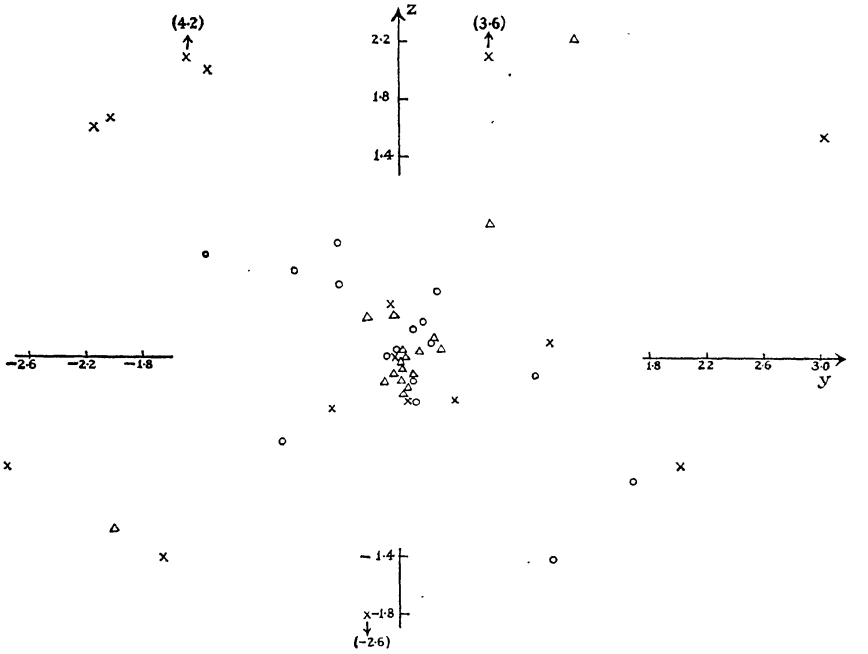

(*c*) $\tau = 0{\cdot}80$.

FIG. 7.—*Structural developments in the yz-plane of V-shaped cluster with halo.*

respectively, for the heavy and light masses. At the time of minimum contraction the values are 108 and 80 in spite of the large g-value ($g \sim 0{\cdot}78$). The reason for this is that the contraction causes bodies in the inner regions to acquire a higher potential energy and this is not compensated by a corresponding increase in the general force field. After a while the mean binding energies decline again, at $\tau \sim 0{\cdot}59$ the respective values are 64 and 52. Binding energies for the central sub-clusters, however, are considerably higher than the mean throughout.

The departures from equilibrium as discussed in Section 5 are larger still for the irregular clusters. For the V-shaped cluster $\Lambda_{\max} \sim 42$ per cent and $\Lambda > 0$ in the range $0{\cdot}17 < \tau < 0{\cdot}73$, whereas $\Lambda_{\max} \sim 55$ per cent in the second case and also $\Lambda > 0$ during most of the time. The maximum departures occur at the time for minimum contraction, but large values of Λ are also found at later times and is partly due to errors. These results show that even for $N = 50$ one may have appreciable deviations in the mean mass if it is assumed that $\Lambda = 0$.

It has been mentioned that some of the radial kinetic energy is converted into tangential motion, and some results will be quoted. At the time of minimum contraction for the V-shape ($\tau \sim 0{\cdot}24$) we find $\langle v_t \rangle / \sqrt{2} \sim 2{\cdot}5$ and $\sim 1{\cdot}8$ for $m = 0{\cdot}50$ and $m = 1{\cdot}50$, respectively, whereas for both mass groups $\langle v_r \rangle \sim 9{\cdot}0$. At the end of the integrations ($\tau \sim 0{\cdot}80$) the bodies within $r = 0{\cdot}40$ have $\langle v_t \rangle / \sqrt{2} \sim 3{\cdot}9$, whereas $\langle v_r \rangle \sim 4{\cdot}9$. This shows that already the system has achieved a fair degree of equipartition in the different modes of motion since the time of minimum contraction. For the elliptical cluster at minimum contraction ($\tau \sim 0{\cdot}29$) $\langle v_t \rangle / \sqrt{2} \sim 5{\cdot}4$ and $\sim 4{\cdot}0$, respectively for $m = 0{\cdot}50$ and $m = 1{\cdot}50$, whereas $\langle v_r \rangle \sim 10{\cdot}0$ and $\sim 8{\cdot}5$. That is, the tangential components are relatively stronger in this case. At the end of the integrations the 18 bodies within $r = 0{\cdot}40$ have $\langle v_t \rangle / \sqrt{2} \sim 4{\cdot}4$ while $\langle v_r \rangle \sim 3{\cdot}2$. Since these results may be somewhat unreliable

because of the errors the same quantities are evaluated at $\tau \sim 0{\cdot}59$. It turns out that $\langle v_t \rangle / \sqrt{2} \sim 4{\cdot}3$ and $\langle v_r \rangle \sim 3{\cdot}6$, hence there seems to be a real dominance of tangential velocity in this sub-cluster.

The main conclusions for the two different clusters are:

(i) the degree of flattening is maintained;

(ii) tangential velocities are generated from purely radial motion;

(iii) stable sub-systems are formed.

The resulting sub-clusters are formed during the initial contraction, and apart from being central they are also highly compact. On the average about 20 bodies of relatively high binding energy are confined within $r \sim 0{\cdot}40$. Thus the sub-cluster radii would correspond to ~ 100 kpc on the standard model for $N = 50$, with times of stability exceeding $\sim 4 \times 10^9$ yrs and $\sim 6 \times 10^9$ yrs, respectively.

A small number of galaxy clusters have been observed where the main mass appears to be contained within a small central region (**11**). It is interesting to speculate that such systems might have been formed during a stage of radial contraction. The possibility also exists, however, that the supercompact clusters are dynamically very old, showing a dense nucleus within a dispersed halo.

10. *Interactions with field galaxies.*—It is often difficult for an observer to decide whether a particular object is a cluster member or just happens to lie in the line of sight to the cluster. Field galaxies are moving about at random and it seems likely that some may move through clusters and ineract with the bound cluster members. The presence of the clusters will actually increase the probability for interactions because of the central field effect on the random motions. In a region with 1 field galaxy per cluster volume one might expect that at least 4 may move through a typical cluster during $\sim 10^{10}$ yrs. As a typical cluster we use the data from $N = 50$, $h = 0$, at $\tau = 1{\cdot}00$ so as to have a partially relaxed system. This offers the advantage of a direct comparison until $\tau \sim 1{\cdot}75$.

The velocity of a free body can be written as

$$\tfrac{1}{2} v_f^2 \sim \frac{N}{r} - E_f \tag{38}$$

where E_f is the free energy w.r. to the cluster centre and the potential $\sim N/r$. The mean binding energy per unit mass ~ 25 for $N = 50$. It would therefore seem reasonable as a first attempt to take $E_f \sim -25$, this gives $v_f \sim 8{\cdot}7$ for an orbit at the distance $r = 4$. Masses and coordinates for the 4 field bodies are $m = 0{\cdot}50$ $z = \pm 4$, and $m = 2{\cdot}0$, $y = \pm 4$, so that for simplicity the free bodies move in radial orbits initially.

After an integration time $\tau \sim 0{\cdot}75$ all the 4 free bodies have moved through the cluster so that again $r \sim 4$. For the group as a whole there is only a slight loss of free energy, but the individual bodies have suffered relatively large changes. Unfortunately, the free bodies themselves appear to have had close encounters with each other near the cluster centre, and there may be some doubts about the accuracy of these integrations. Before this happened, however, 3 of the 4 bodies had given up 15–30 per cent of their free energy to the cluster members.

21 of the 50 cluster members show significant changes in position with

$$\langle |\Delta \mathbf{r}| \rangle \sim 0{\cdot}60.$$

The normal increase in the moment of inertia for the bound cluster is halted around $\tau \sim 1{\cdot}50$, and it remains constant until $\tau \sim 2{\cdot}22$ when the integration is terminated. This is due to the four bodies moving essentially in a plane and through the central region, thereby producing a net inward force component on the more distant bodies.

As a second case we take $v_f = 6{\cdot}0$ at the same distance; this increases the probability of interaction with the cluster members considerably, because the relaxation time is proportional to v_f^3. The coordinates and velocities chosen for the four field galaxies give impact parameters w.r. to the cluster centre $\sim 1{\cdot}0$–$1{\cdot}5$ and the total motion is not confined to one plane only. Table IX shows the binding energies for the four free bodies at various times (initially $\tau = 1{\cdot}00$). Closest approach to the cluster centre is made around $\tau \sim 1{\cdot}55$ when the distances are $\sim 0{\cdot}5$–$1{\cdot}0$. All four bodies show significant interactions with the cluster members. There is a net loss of free energy to the cluster from three field bodies and this is equivalent to the mean binding energy of one cluster member with unit mass. The importance of the energy loss depends on the way in which it is distributed to the cluster members. If the extra energy is given to a small number of light bodies it will have the effect of increasing the mean distances considerably. The high relative velocities, however, do not allow much time for a large energy exchange between individuals. It therefore seems probable that the general effect will be a slight decrease in the binding energies of many bodies without any important structural changes. This is confirmed when we make a comparison with the case where there is less interaction with the free bodies.

TABLE IX

The binding energy of field galaxies interacting with a cluster

τ	$E_1(m=2)$	$E_2(m=2)$	$E_3(m=0{\cdot}5)$	$E_4(m=0{\cdot}5)$	τ	E_1	E_2	E_3	E_4
1·00	−5·0	−5·4	−4·3	−4·5	1·74	4·6	−5·3	−1·8	−7·8
1·31	−4·4	−4·8	−3·7	−4·7	1·80	5·9	−4·7	−1·8	−7·7
1·49	0·3	−1·6	−7·0	−4·4	1·93	6·5	−4·1	−1·9	−7·4
1·56	1·4	−2·3	−8·3	−5·5	2·32	6·2	−4·0	−2·0	−7·3
1·62	4·8	−5·4	−2·2	−6·8	2·65	5·7	−4·1	−2·1	−7·3

The moment of inertia of the originally bound cluster levels out at $\tau \sim 1{\cdot}70$, this is somewhat later than in the previous case but is due to the smaller velocities of the free bodies. I stays approximately constant until $\tau \sim 2{\cdot}30$, whereupon there is a slow increase again. Even so, the final value $I \sim 139$ at $\tau \sim 2{\cdot}65$ is smaller than would be expected for the undisturbed cluster. This means that the free bodies have again acted on the more distant bodies with a net inward force component.

One could regard the free bodies around $\tau \sim 1{\cdot}55$ as belonging to the cluster and in the process of being ejected. In order that a body shall escape the cluster it is not sufficient that $E_i < 0$ since further encounters may lead to a loss of the free energy. The mean free path is of the order of 30 mean cluster radii for $N = 50$ and the velocity of escape (**3**); it is not surprising, therefore, that one of the bodies did not manage to escape. This also happened for one body in the case of the elliptical cluster. The retardation of escaping stars has been considered by King (**14**) who

finds that the effective time of relaxation is increased by ~ 17 per cent for $N=50$ and a centrally concentrated model. The preliminary investigation reported in this paper therefore appears consistent with theory.

11. *The ϵ-effect.*—All discussions of results have so far been based on integrations where the quantity ϵ has been included. Since the force acting on a body is modified significantly when the distance to a neighbour $\sim\epsilon$ it is to be expected that this factor has some effect on the overall dynamical evolution. The general force field is weakened by the inclusion of ϵ and this indicates that mean distances should be slightly smaller for systems near equilibrium.

TABLE X

The effect of ϵ on the moments of inertia: $N=50$ ($\eta=1/10$)

$\epsilon=10^{-10}$				$\epsilon=0.04$			
τ	I_x	I_y	I_z	τ	I_x	I_y	I_z
0·246	42·8	41·9	32·1	0·241	42·4	41·5	32·0
0·339	44·3	43·9	37·4	0·344	43·3	44·0	37·6
0·492	43·2	46·3	50·0	0·493	40·9	47·3	50·3

The cases $N=50$, $g=0.50$, $\epsilon=0.04$ and $\epsilon=10^{-10}$ are compared in Table X where the three moments of inertia are given. The overall situation appears to be much the same but the relatively small integration times does not allow a final conclusion to be made. When individual positions are compared we find that the deviations are appreciable in some cases. Thus at $\tau\sim 0.49$ there are 15 bodies with $|\Delta\mathbf{r}|\gtrsim 0.15$, and $\langle|\Delta\mathbf{r}|\rangle\sim 0.60$ for these. On the other hand, there are bodies for which $|\Delta\mathbf{r}|\sim 0.01$ only, even if they do not belong to the halo population. The number of close encounters with impact parameters $\lesssim 2\epsilon$ is probably sufficient to explain the large deviations in position. The production of low-energy bodies, however, do not appear to be significantly different in the two cases.

Initially, the forces and velocities are slightly different in the two cases. The dynamical history of a body before its first encounter may therefore depend on ϵ and this would result in a different encounter. This is clearly a statistical effect not significant when long-term evolution is considered. We may therefore conclude that the inclusion of a cut-off parameter in the equations of motion would seem to reproduce well the dynamical conditions in galaxy clusters. Furthermore, the general features of star cluster evolution may be described by the same results. The dynamical evolution *rate*, however, is likely to be somewhat slower when ϵ is included.

The choice of ϵ effectively determines a length scale for the clusters, whereas the time scale only becomes fixed when the total mass is given. For $N=100$ we take $\epsilon=0.03$; this corresponds to an effective galaxy radius $\xi\sim 10$ kpc (eqn. 4*b*) on the basis of the standard model. A homologous scaling then gives $\epsilon\sim 0.04$ for $N=50$.

12. *Method for numerical solution.*—The method for choosing the time-steps when integrating the equations of motion is a vital one, as it can easily lead to excessive demands on the machine time. In the method used by von Hoerner (**2**) the two closest bodies determine the time-step for the rest. The time to compute the total force on one body is approximately equal to the time to integrate all velocities and coordinates one step. A method that can limit the number of force computations will therefore save machine time and allow one to deal with higher values of N.

We will take the relative variation in total force as the essential criterion for the time-step computation. Bodies in regions of the cluster where the variation in force is relatively small will therefore be allowed to move a longer distance before recomputations of force are necessary. A maximum value for the permissible time-step will be used in order that future encounters shall not be missed. The time-step criterion is taken to be

$$\Delta\tau_i = \eta \min\left[\frac{1}{N}, \frac{F_i^2}{\dot{F}_i^2} + \delta^2\right]^{1/2} \tag{39}$$

where $\mathbf{F}_i$ is the total force per unit mass acting on the ith body, and δ is a small quantity included to avoid $\Delta\tau_i \sim 0$ in the exceptional case $|\mathbf{F}_i| \sim 0(\delta = 10^{-5})$. The numerical factor η determines the accuracy to which we want to integrate, and will be decided by trial integrations. Eqn. (39) gives $\Delta\tau_{\max} = \eta N^{-1/2}$ for the maximum time-step; this is related to the crossing time by eqn. (21) and we have

$$\Delta\tau_{\max} \sim 0{\cdot}2\,\eta\tau_{\mathrm{cr}}. \tag{40}$$

Normally the time-step will be determined by the second quantity in the bracket of (39), this means that relative errors in position will be of the same order of magnitude. The total force acting on a body changes by a factor $\sim\eta$ during an integration step, and in order to use η as large as possible one can include higher-order terms in the force. We take a Taylor series with three terms in the force, viz.

$$\mathbf{F}_i(\tau_i') = \mathbf{F}_i(\tau_i) + \frac{d\mathbf{F}_i(\tau_i)}{d\tau}\Delta\tau_i + \tfrac{1}{2}\frac{d^2\mathbf{F}_i(\tau_i)}{d\tau^2}\Delta\tau_i^2 \tag{41}$$

where $\Delta\tau_i = \tau_i' - \tau_i$ is determined by (39).

Initially, $\mathbf{r}_i$, $d\mathbf{r}_i/d\tau$, and $\mathbf{F}_i$ are known and this information is used to integrate the equations of motion a small fixed step $\Delta_1\tau$ for all bodies. New forces are then computed at $\tau_i = \Delta_1\tau$, and individual time-steps are determined by (39). From the knowledge of $d\mathbf{F}_i/d\tau$ at $\Delta_1\tau$ we then correct $\mathbf{r}_i$ and $d\mathbf{r}_i/d\tau$ to this order. All coordinates, velocities, and forces are now given increments according to (41) where only the two first terms are known at $\tau_i = \Delta_1\tau$, viz.

$$\left.\begin{aligned} \Delta\bar{\mathbf{r}}_i &= \frac{d\mathbf{r}_i(\tau_i)}{d\tau}\Delta\tau + \tfrac{1}{2}\mathbf{F}_i(\tau_i)\Delta\tau^2 + \tfrac{1}{6}\frac{d\mathbf{F}_i(\tau_i)}{d\tau}\Delta\tau^3 \\ \Delta\left(\frac{d\bar{\mathbf{r}}_i}{d\tau}\right) &= \mathbf{F}_i(\tau_i)\Delta\tau + \tfrac{1}{2}\frac{d\mathbf{F}_i(\tau_i)}{d\tau}\Delta\tau^2 \\ \Delta\mathbf{F}_i &= \frac{d\mathbf{F}_i(\tau_i)}{d\tau}\Delta\tau \end{aligned}\right\} \tag{42}$$

where $\Delta\tau = \min_i(\Delta\tau_i)$ and the barred quantities indicate that the third term in the force equations has not yet been included.

At time $\tau_\alpha = \Delta_1\tau + \Delta\tau_\alpha$ the force is computed for the body $i = \alpha$ and eqns. (42) are updated to include $d^2\mathbf{F}_\alpha/d\tau^2$;

$$\left.\begin{aligned} \Delta\mathbf{r}_\alpha &= \Delta\bar{\mathbf{r}}_\alpha + \frac{1}{24}\frac{d^2\mathbf{F}_\alpha(\tau_\alpha)}{d\tau^2}\Delta\tau_\alpha^4 \\ \frac{\Delta\mathbf{r}_\alpha}{d\tau} &= \Delta\left(\frac{d\bar{\mathbf{r}}_\alpha}{d\tau}\right) + \frac{1}{6}\frac{d^2\mathbf{F}_\alpha(\tau_\alpha)}{d\tau^2}\Delta\tau_\alpha^3. \end{aligned}\right\} \tag{43}$$

Furthermore, the new time-step for this body is computed. To apply the method of individual time-steps we use three tables of time for each body:

(i) time at which force was last computed (τ_i);

(ii) portion of step remaining before new force computation is needed; viz. $\Delta\tau_i' = \Delta\tau_i - \sum\Delta\tau$. When $\Delta\tau_i' = 0$, $i = \alpha$ and $\Delta\tau_i'$ is replaced by the new step;

(iii) the time-step $\Delta\tau_i$ needed by eqns. (43).

In the subsequent integration the time-steps used by eqns. (42) are given by $\Delta\tau = \min_i(\Delta\tau_i')$, and eqns. (43) are used for $i = \alpha$ only.

No accuracy is lost by splitting $\Delta\tau_i$ into many smaller steps when $\mathbf{F}_i$ is updated after each small step. The velocities and coordinates are therefore known at any time to the accuracy of $d\mathbf{F}_i/d\tau$, and at the end of each step $\Delta\tau_i$ to the accuracy of $d^2\mathbf{F}_i/d\tau^2$.

13. *Error analysis.*—This problem is of such a nature that accurate solutions are neither possible in practice nor necessary. What is desired, however, is that the solutions shall be sufficiently convergent to exclude serious errors. It is convenient to distinguish between errors of two kinds:

(i) errors in total energy and angular momentum;

(ii) errors in velocity and positions for each body.

In dealing with large systems it is sufficient to keep a control of errors of the first kind, provided one has carried out some test cases trying to correlate (i) and (ii). Errors produced by different values of the time-step factor η are not related in a simple way. Apart from statistical fluctuations the errors should tend to become saturated, expressing the convergence of the solutions. It is therefore important to know the value of η when further improvements will not yield much in relation to the extra time needed.

Integrations can only be carried out satisfactorily as long as the centre of mass does not depart significantly from the origin of the coordinate system. The actual deviation is defined by

$$\Delta\mathbf{r}_G = \frac{1}{N}\sum_{i=1}^{N} m_i\mathbf{r}_i. \tag{44}$$

Similarly, $d\mathbf{r}_G/d\tau$ is also computed and these quantities are printed together with the main control line. If the mean errors in position, $\langle|\Delta\mathbf{r}_i|\rangle$, were distributed at random we would have

$$\langle|\Delta\mathbf{r}_i|\rangle \sim \sqrt{N}\Delta r_G. \tag{45}$$

Total error in energy is defined by

$$\Delta E_{\text{tot}} = \sum_{k=1}^{P} |E_k - E_{k-1}| \tag{46}$$

where E_0 is the initial value of the total energy and the energy check is done P times. The error defined in this way will therefore be larger than the maximum deviation from E_0 ($\Delta E_{\max} \sim 1/3\Delta E_{\text{tot}}$). Table XI contains $\Delta E_{\text{tot}}/E_0$ and Δr_G for the case $N = 50$, $\epsilon = 0{\cdot}04$, $h = 0$, for three trial values of η.

TABLE XI

Trial integrations with different step-lengths: $N=50$

	$\Delta E_{tot}/E_0$			Δr_G		
τ	$\eta=1/5$	$\eta=1/7$	$\eta=1/10$	$\eta=1/5$	$\eta=1/7$	$\eta=1/10$
0·34	...	0·6 per cent	0·4 per cent	...	0·0008	0·00016
0·37	1·2 per cent	...	...	0·003	...	...
0·55	1·6	0·8	...	0·006	0·0019	...
1·00	2·2	...	...	0·019	...	...
1·75	9·0	...	...	0·055	...	...

When individual positions are compared it is found that $\eta=1/5$ gives rise to some unsatisfactory cases; this is due to close encounters not being detected early enough for the time-step to be shortened. On the other hand, the differences between $\eta=1/7$ and $\eta=1/10$ does not seem significant enough to justify an extra 43 per cent in the machine time. It is found that with $\eta=1/10$ as a standard, the absolute errors in position for the poorest cases $\lesssim 0{\cdot}015$ for $\eta=1/7$ at $\tau=0{\cdot}34$. It is to be expected that the accumulation of errors in position will increase faster than linearly with time. This appears to be confirmed by the values of Δr_G in Table XI. The general force field varies more smoothly with increasing N, hence the same value of η should actually lead to better integrations for equivalent physical times. The value $\eta=1/7$ is therefore adopted for $N=50$ and $N=100$ when the systems are stable. A contracting system will develop high velocities and the integrations for the V-shaped cluster was therefore started with $\eta=1/7$, but at $\tau\sim 0{\cdot}29$ when $\Delta E_{tot}/E_0\sim 7$ per cent a switch was made to $\eta=1/10$. In this case we find in all $\Delta E_{tot}/E_0\sim 16$ per cent and the energy is decreasing nearly all the time. Unfortunately, such a precaution was not taken for the contracting elliptical cluster.

When studying Table XI one should bear in mind that even if forces are allowed to change by a factor η, the first and second derivatives are taken into account. The resulting gain in accuracy is considerable, as shown by von Hoerner (**2**).

TABLE XII

Actual integration errors at approximately homologous times

				$h=0$		$h>0$	
N	τ	η	$\Delta E_{tot}/E_0$	Δr_G	$\Delta J_{tot}/J_0$	Δr_G	$\Delta J_{tot}/J_0$
100	0·87	1/7	2·0 per cent	0·010	5·4 per cent	0·016	4·5 per cent
50	1·22	1/7	...	...	...	0·014	4·4
25(I)	1·83	1/10	...	...	...	0·019	3·6
25(II)	2·04	1/12	0·8	...	1·8	0·004	1·3

In Table XII we give data relevant to the discussion of errors for the cases $N=100$, 50 and 25, both for $h=0$ and $h>0$. (For maximum errors in energy cf. Table IV.) The angular momentum check is not included in the test cases, but ΔJ_{tot} is defined in the same manner as ΔE_{tot}. The total deviations in energy do not seem unduly large in relation to the values of the integration times. The values of Δr_G are related to the mean errors in position by (45). When the total angular momentum is small one should rather compare ΔJ_{tot} to $\langle|\mathbf{J}_i|\rangle$; from this we find that $\Delta J_{tot}/N$ represents ~ 1 per cent of the mean angular momenta for the two large clusters.

In concluding the error analysis it should be emphasized that we are primarily interested in the dynamical behaviour of the clusters as a whole. The qualitative conclusions drawn from the integrations should therefore not be significantly affected by the numerical errors involved. If substantially larger clusters are integrated by the present method the number of small integration steps may become large enough for rounding-off errors to contribute.

14. *Time-step considerations.*—The effectiveness of the method of individual time-step integration can be tested on the integration of close encounters. It is essential that the encounters are detected in time in order to avoid over-shooting. When close encounters are examined in detail it is found that for $N = 100$, $\eta = 1/7$ only a few cases show relatively large variations in $\Delta\tau_i$.

For very close encounters, including collisions ($r_{12} \sim \epsilon$), typical values of the time-steps $\sim 3 \times 10^{-4}$; on the standard model this would then correspond to $\sim 3 \times 10^6$ yrs. Averaging over the whole integration period $\langle \Delta\tau_i \rangle \sim 0{\cdot}0056$ for the lightest mass group, and the value is declining to $\sim 0{\cdot}0032$ for $m = 3{\cdot}75$. This means that the average steps would represent times $\sim 3 \times 10^7$ yrs–$5{\cdot}5 \times 10^7$ yrs, whereas the maximum steps would be equivalent to $\sim 14 \times 10^7$ yrs. R.m.s. velocity $\sim 6{\cdot}5$ and typical velocities during close encounters ~ 9–13. The velocity unit based on the standard model is ~ 36 km sec^{-1}, hence $(\langle v^2 \rangle)^{1/2} \sim 230$ km sec^{-1} when the virial theorem is satisfied.

On the average nearly half the number of bodies move with the maximum permitted time-step, and about 20 per cent of these have $r \lesssim 1$. The high proportion of maximum time-steps shows that the mean spacing is fairly large compared to the distances travelled during this time. Nearly all close encounters take place within $r \sim 1$, while encounters in the outer regions are more easily detected because of the smaller shielding of other close bodies. In view of this it would seem possible to save some computing time by modifying $\Delta\tau_{\max}$. For example, we may take

$$\Delta\tau_{\max} = \frac{\eta}{\sqrt{N}} r \tag{47}$$

for $r > 1$. For a body travelling with r.m.s. velocity we would then have $v\Delta\tau_{\max} \sim 0{\cdot}10\, r$ for $\eta = 1/7$, and this would seem good enough when there are three terms in the force expansion.

A considerable proportion of the machine time is taken up by the close encounters. After each small step the total forces on the close bodies are recomputed, even though the changes in the background forces are small in most cases. As a possible method of further time saving one could keep the background force constant during the closest part of the encounters when there will be many small steps. This would not be satisfactory, however, in cases of many-body encounters. Since the number of such encounters is relatively small one could then integrate by the usual method.

Finally, the method for time-step computation could be extended to include the relative value of the first and second force derivatives as well; this would improve the accuracy for critical cases without demanding much additional time.

15. *Machine time estimates.*—It is very useful to have a good estimate of the time required by the computer to integrate a system of N bodies for a certain value of the scaled time. The machine time equation can be written as

$$T_m = T_0 + AP + B'N\mathcal{N}(\tau) + C'\mathcal{N}(\tau) \tag{48}$$

where T_0 is the time to read the programme and data into the computer and perform the initial scalings and corrections. A is the time to compute the main control line and do the averaging, and this is done P times. The time to compute the force on one body and integrate all velocities and coordinates one step is included in the third term, and this is done $\mathcal{N}(\tau)$ times. The last term is optional and C' represents the time to write one line of results on magnetic tape.

It is more convenient to express $\mathcal{N}(\tau)$ by τ since this relates to the physical time. This can only be done when the relation between mean step and maximum step is known. It turns out that the ratio f between these are very nearly the same for $N=50$ and $N=100$ when semi-stationary systems are integrated. We have (cf. (39))

$$\langle \Delta\tau_i \rangle = f\Delta\tau_{\max} = \frac{f\eta}{\sqrt{N}}. \tag{49}$$

The number of small steps $\Delta\tau$ in time τ is then

$$\mathcal{N}(\tau) \sim \frac{N\tau}{\langle \Delta\tau_i \rangle} = \frac{N^{3/2}\tau}{f\eta}. \tag{50}$$

Using $\eta = 1/7$ and $N=100$ when the constants in eqn. (48) are determined the general machine time equation becomes

$$T_m = T_0 + AP + \frac{1}{7\eta}\left(\frac{N}{100}\right)^{3/2}\left[\frac{BN}{100} + C\right]\tau \tag{51}$$

where $B = 7\times 10^5 f^{-1} B'$ and $C = 7\times 10^3 f^{-1} C'$.

The constants T_0 and A are determined directly; the respective values are ~ 45 secs, 3 secs for $N=50$ and ~ 105 secs, 8 secs for $N=100$. From two long integrations we find $B \sim 60$ mins, $C \lesssim 3$ mins. The final form of (51) gives good agreement with other cases. The effective computing time (in minutes) is

$$T_c \sim \frac{60}{7\eta}\left(\frac{N}{100}\right)^{5/2}\tau. \tag{52}$$

It therefore appears that the method depends on the factor $N^{5/2}$, but scaled time and physical time are related by a factor $N^{1/2}$ for homologous systems (eqn. 25); this makes $T_c \sim N^2 t$ where t is the physical time. The general relation between T_c and t is given by a combination of eqns. (52) and (4*a*). In the method used here the time T_c is divided between force computations and integrations in the approximate ratio 3 : 4.

The above time considerations apply to the I.B.M. 7090 computer with a fundamental machine cycle $2{\cdot}2\times 10^{-6}$ sec. The present method uses $\lesssim 5$ fundamental cycles per mean instruction, that is, eqn. (52) is based on a computer speed of $\sim$ 100,000 mean operations per sec.

Acknowledgments.—The author gratefully acknowledges a generous grant from the Department of Scientific and Industrial Research for the computational work.

I am greatly indebted to Professor F. Hoyle for suggesting this problem and for his close co-operation in developing the computer programme. It is a pleasure to record discussions with Professor A. Schlüter who suggested the method of individual time-step integration. Thanks are also due to Dr. D. Lynden-Bell for helpful comments on the contents of this paper.

APPENDIX

Let two bodies of masses m_1 and m_2 at mean distance r suffer an equal and opposite energy exchange ΔE and call the new mean distances r_1 and r_2. The resulting change in moment of inertia is

$$\Delta I = m_1(r_1^2 - r^2) + m_2(r_2^2 - r^2). \tag{1}$$

Call the corresponding changes in potential $\Delta_1\Phi$ and $\Delta_2\Phi$, hence

$$|\Delta E| = m_1 |\Delta_1\Phi| = m_2 |\Delta_2\Phi| \tag{2}$$

Φ is considered known and we seek a relation between ΔI and Φ. Eqn. (1) suggests that ΔE be expanded in terms of r^2. The two first terms are

$$\Delta E = m_1 \frac{\partial\Phi}{\partial(r^2)} \Delta_1 r^2 + \frac{m_1}{2} \frac{\partial^2\Phi}{\partial(r^2)^2} \Delta_1 r^4 \tag{3}$$

where $\Delta_1 r^2 = r_1^2 - r^2$. By writing a similar expression for m_2 with $\Delta_2 r^2 = r_2^2 - r^2$ and adding we get

$$\Delta I = \frac{Q r \, \partial^2\Phi/\partial(r^2)^2}{-\dfrac{\partial\Phi}{\partial r}} \tag{4}$$

with $Q = m_1\Delta_1 r^4 + m_2\Delta_2 r^4$.

Since $-\partial\Phi/\partial r > 0$ for all distributions the sign of ΔI depends on $\partial^2\Phi/\partial(r^2)^2$, that is, on the expression

$$4r^2 S = \frac{\partial^2\Phi}{\partial r^2} - \frac{1}{r}\frac{\partial\Phi}{\partial r}. \tag{5}$$

Poisson's equation for a spherical distribution is

$$\frac{\partial^2\Phi}{\partial r^2} + \frac{2}{r}\frac{\partial\Phi}{\partial r} = -4\pi G\rho(r). \tag{6}$$

Substituting $\partial^2\Phi/\partial r^2$ from (6) into (5) then gives

$$4r^2 S = -4\pi G\rho(r) - \frac{3}{r}\frac{\partial\Phi}{\partial r}. \tag{7}$$

We also have

$$-\frac{\partial\Phi}{\partial r} = \frac{GM(r)}{r^2} = \frac{4\pi G}{3}\langle\rho(r)\rangle r. \tag{8}$$

Hence

$$S = \frac{\pi G}{r^2}[\langle\rho(r)\rangle - \rho(r)] \tag{9}$$

and $S > 0$ for $\rho(r)$ declining with r. This condition is satisfied in all real clusters, and we therefore have that

$$\Delta I = \frac{3Q}{4r^2}\left[1 - \frac{\rho(r)}{\langle\rho(r)\rangle}\right] > 0. \tag{10}$$

This proof is only strictly true when the bodies are in circular orbits and as long as (3) is a good approximation, but energy considerations indicate that the moment of inertia will also increase in the general case.

Department of Applied Mathematics and Theoretical Physics,
Cambridge University,
Cambridge:
1962 *November.*

References

(1) Abell, G. O., *Ap. J. Supp.*, **3,** 211, 1958.
(2) von Hoerner, S., *Zs. f. Astrophys.*, **50,** 184, 1960.
(3) Chandrasekhar, S., *Principles of Stellar Dynamics* (Dover edition), p. 204, 1960.
(4) Limber, D. N., Santa Barbara Conference on the instability of systems of galaxies, *A.J.*, **66,** 572, 1961.
(5) Chandrasekhar, S., *Ibid.*, p. 259, 1960.
(6) Baade, W., and Spitzer, L., *Ap.J.*, **113,** 413, 1951.
(7) Page, T., Santa Barbara Conference, *A.J.*, **66,** 614, 1961.
(8) Hoyle, F., *M.N.*, **105,** 40, 1945.
(9) Vorontsov-Velyaminov, B. A., *Atlas of Peculiar Galaxies* (Moscow, 1960).
(10) Burbidge, E. M., and Burbidge, G. R., *Ap. J.*, **130,** 629, 1959.
(11) van den Bergh, S., Santa Barbara Conference, *A.J.*, **66,** 568, 1961.
(12) Limber, D. N., *Ap. J.*, **135,** 41, 1962.
(13) King, I., *A.J.*, **63,** 109, 1958.
(14) King, I., *A.J.*, **64,** 351, 1959.